Introduction to XEDS in the AEM

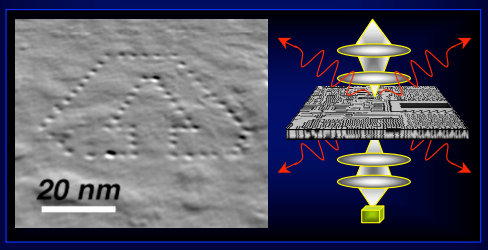

Nestor J. Zaluzec

zaluzec@microscopy.com

zaluzec@aaem.amc.anl.gov

Brief Review of X-ray Generation

Instrumentation: Detector Systems

Instrumentation: EM Systems

Data Analysis and Quantification:

Additional Topics

Brief Review of X-ray Generation

Electron Excitation of Inner Shell & Continuum Processes
Characteristic and Bremsstrahlung Emission
Spectral Shapes
Notation of Lines

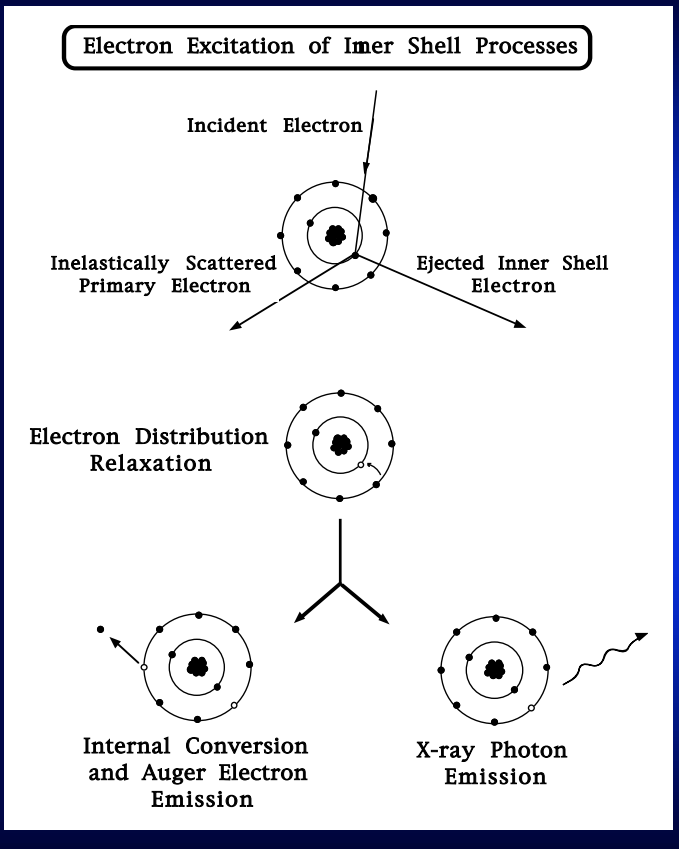

The Emission Process:

1-Excitation,
2-Relaxation,
3-Emission

Nomenclature for Principle X-ray Emission Lines

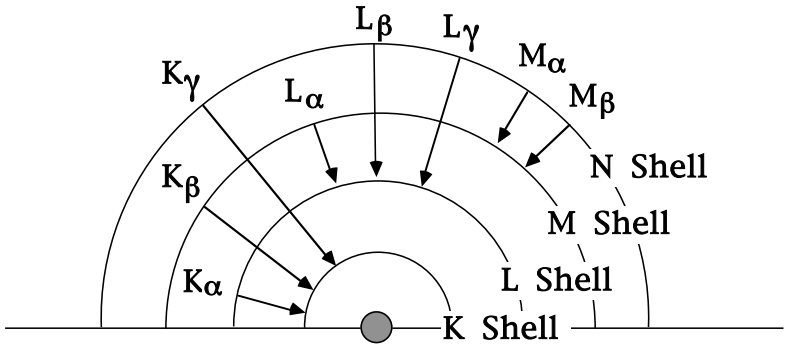

Characteristic X-ray Line Energy = $E_{final} - E_{initial}$

Recall that for each atom every shell has a unique energy level determined by the atomic configuration for that element.

∴ X-ray line energies are unique.

Nomenclature for X-ray Lines

X-ray Transition Selection Rules: (Principle Quantum Numbers)

Shell	n	l	j	Rule
K	1	0	1/2	
L	2	0,1	1/2, 3/2	Δn >0
M	3	0,1,2	1/2, 3/2, 5/2	Δl = +1, -1
N	4	0,1,2,3	1/2, 3/2, 5/2, 7/2	Δj = +1, 0, -1

Relative Intensities of Major X-ray Lines

$K_{\alpha 1}$	= 100	$L_{\alpha 1}$	= 100	$M_{\alpha 1,2}$	= 100
$K_{\alpha 2}$	= 50	$L_{\alpha 2}$	= 50	M_{β}	= 60
$K_{\beta 1}$	= 15-30	$L_{\beta 1}$	= 50		
$K_{\beta 2}$	= 1-10	$L_{\beta 2}$	= 20		
$K_{\beta 3}$	= 6-15	$L_{\beta 3}$	= 1-6		
		$L_{\beta 4}$	= 3-5		
		$L_{\gamma 1}$	= 1-10		
		$L_{\gamma 3}$	= 0.5-2		
		L_{η}	= 1		
		L_{ι}	= 1-3		

Relative Intensities of Major X-ray Lines

$$I_K = I_{K\alpha} + I_{K\beta}$$
$$I_L = I_{L\alpha} + I_{L\beta} + I_{L\iota} + I_{L\eta} + I_{L\gamma}$$
$$I_M = I_{M\alpha} + I_{M\beta}$$

Line	Initial	Final	Line	Initial	Final	Line	Initial	Final
$K_{\alpha 1}$ =>	L_3	K	$L_{\alpha 1}$ =>	M_5	L_3	$M_{\alpha 1}$ =>	N_7	M_5
$K_{\alpha 2}$ =>	L_2	K	$L_{\alpha 2}$ =>	M_4	L_3	$M_{\alpha 2}$ =>	N_6	M_5
$K_{\beta 1}$ =>	M_3	K	$L_{\beta 1}$ =>	M_4	L_2	M_{β} =>	N_6	M_4
$K_{\beta 2}$ =>	N_2	K	$L_{\beta 2}$ =>	N_5	L_3	M_{γ} =>	N_5	M_3
$K_{\beta 3}$ =>	M_2	K	$L_{\beta 3}$ =>	M_3	L_1			
			$L_{\beta 4}$ =>	M_2	L_1			
			$L_{\gamma 1}$ =>	N_4	L_2			
			$L_{\gamma 3}$ =>	N_3	L_1			
			L_{η} =>	M_1	L_2			
			L_{ι} =>	M_1	L_3			

Characteristic X-Ray Spectrum Illustrating KLM lines

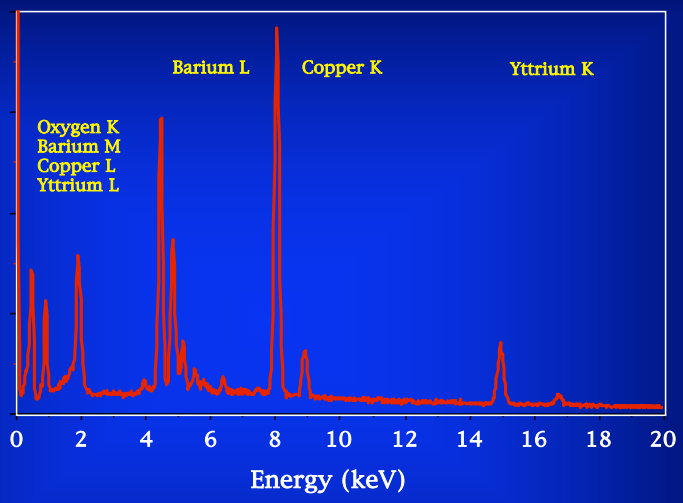

TEM Specimen: $Y_1Ba_2Cu_3O_{6.9}$ Superconductor - 120 kV - UTW Detector

Note:

As Z increases the Kth shell line energy increases.
If K-shell is excited then all shells are excited (Y, Cu, Ba) but may not be detected.
Severe spectral overlap may occur for low energy lines.

Electron Excitation of Continuum Processes

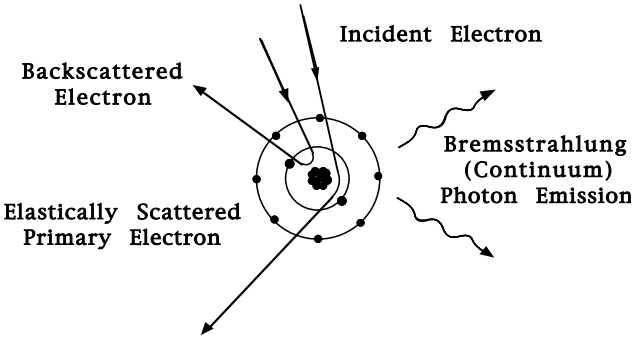

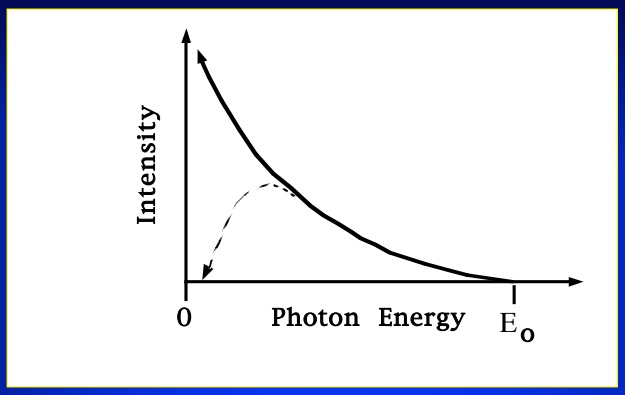

Energy Range - Continuous Distribution

Maximum = Incident Electron Energy (Least Frequent)
Minimum = $E_{plasmon}$ ~ 15-30 eV (Most Frequent)

Spectral Distribution will reflect this range, modified by detector response function

Electron Excitation of Continuum (Background) Intensity

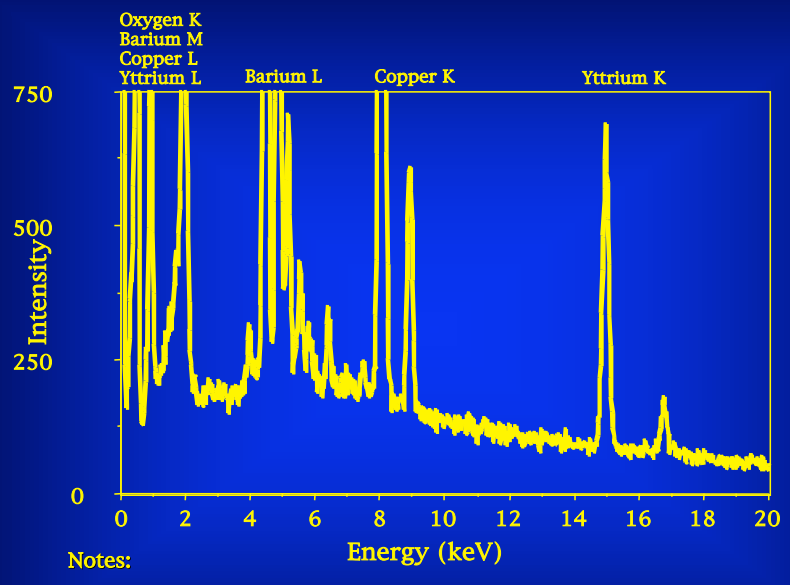

Notes:

Spectral background will be influenced by:
1.) Specimen composition
2.) Detector efficiency
3.) TEM generated artifacts

Instrumentation: Detector Systems

Wavelength Dispersive Spectrometers (WDS)
Energy Dispersive Spectrometers (EDS)
- Si(Li) Detectors
- HPGe Detectors
- Spectral Artifacts of the EDS System
- Detector Efficiency Functions
- Light Element Detectors

Superconducting Calorimeters/Bolometers
Silicon Drift Detectors

Multichannel Analyzers

Energy Dispersive Spectrometers: (Solid State Detector)

Operates on Energy Deposition Principle

Simple, Nearly Operator Independent
Large Solid Angles (0.05-0.3 sr)
Virtually Specimen Position Independent
No Moving Parts
Parallel Detection
Quantification by Standardless or Standards Methods

Poor Energy Resolution (~ 130 eV)
** SuperConducting Systems (~ 20 eV)
Poor Peak/Background Ratios (100:1)
Detection Efficiency Depends upon X-ray Energy

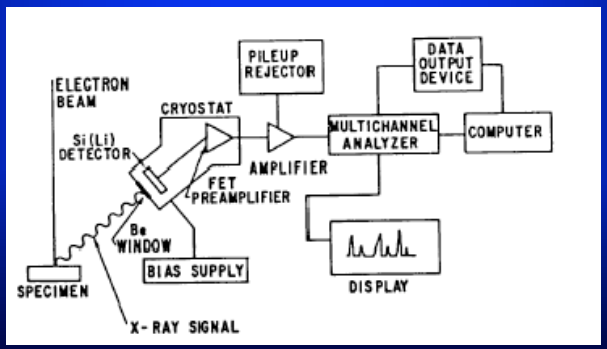

Wavelength Dispersive Spectrometers : (Diffractometer)

Operates using Diffraction Principles (Bragg's Law)

Excellent Energy Resolution (~ 5 eV)
High Peak/Background Ratios (10000:1)
Good Detection Efficiency for All X-rays
High Counting Rates
Good Light Element Capabilities

Complex Mechanical Devices, Operator Intensive
Specimen Height dependant focus
Moving Components in the AEM
Limited Solid Angles (<0.01 sr)
Serial Detection
Quantification Requires Standards

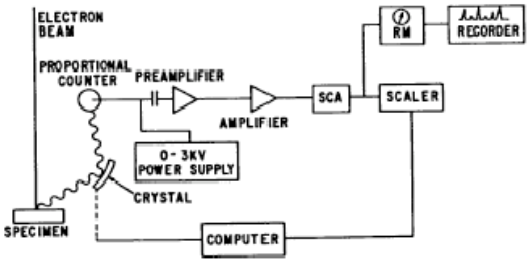

FIGURE 1. Basic components of a crystal diffraction spectrometer system.

Comparison of EDS and WDS Spectrometers

Parameter	Wavelength Dispersive	Energy Dispersive
Construction	Mechanical Device moving components	Solid State no moving parts
Energy Resolution	5 eV	130 eV
Efficiency	$\leq$ 30 %	100 % (3-15keV)
Input Count Rate	30-50 K cps	10 K cps
Peak/Background*	10000	100
Atomic Number Range	Z $\geq$ 4 (Be)	Z $\geq$ 11 (Na) Z $\geq$ 5 (B)
Number of Elements	1 per Detector	All in Energy Range
Solid Angle	0.001-0.01 sr	0.02-0.3 sr
Collection Time	Tens of Minutes	Minutes
Beam Current	High Stability Required	Low Stability Required
Detector Stability	Good Short Term	Excellent
Spectral Artifacts	Neglegible	Important
Operation	Skilled (?)	Novice

* Values depend on definition, specimen, and operating conditions

Comparison of EDS and WDS Spectra

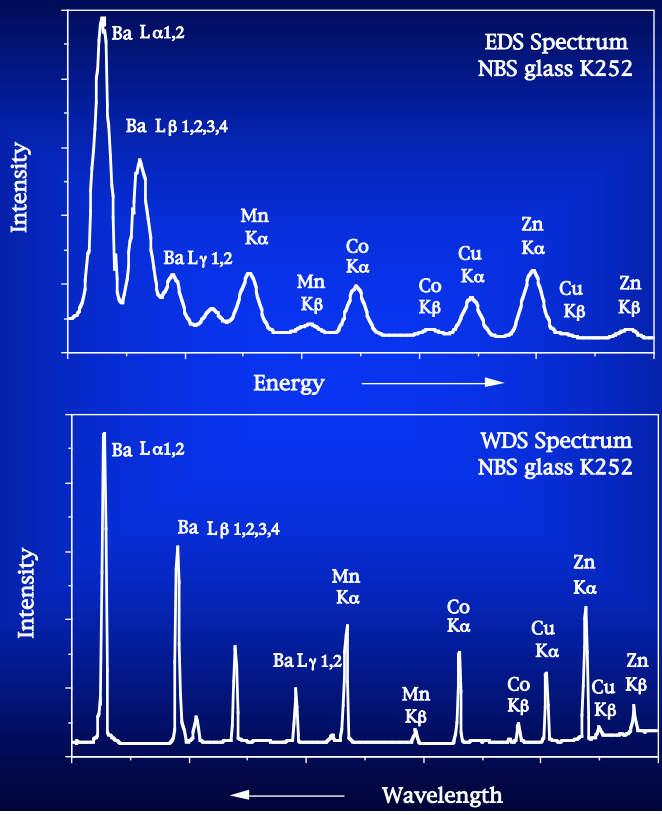

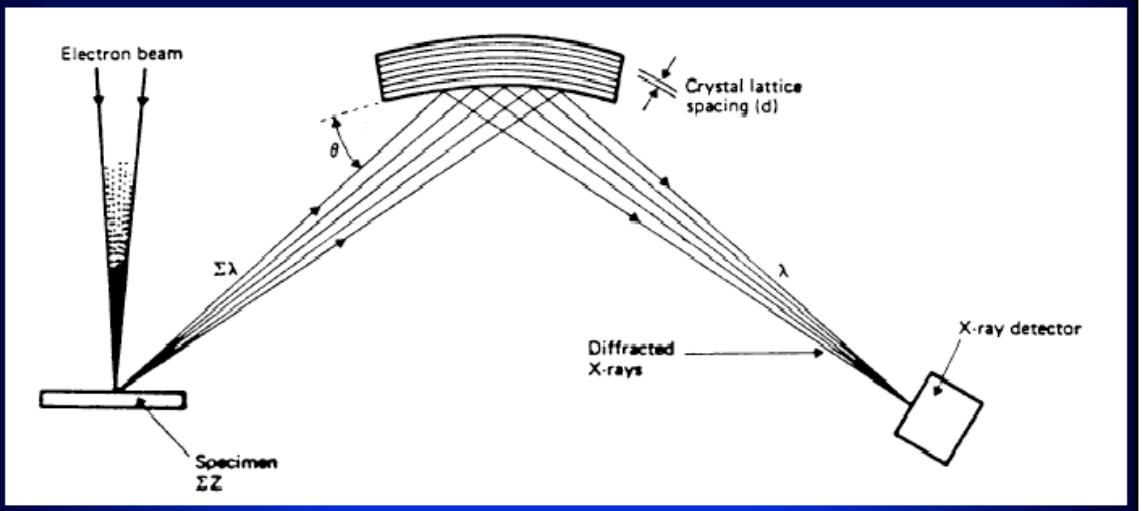

Operation of a Crystal Spectrometer Using Braggs' Law

$$\lambda = 2\,d\,\sin(\theta)$$

$$\lambda = 12.398\ [\text{Å}] / E\ [\text{keV}]$$

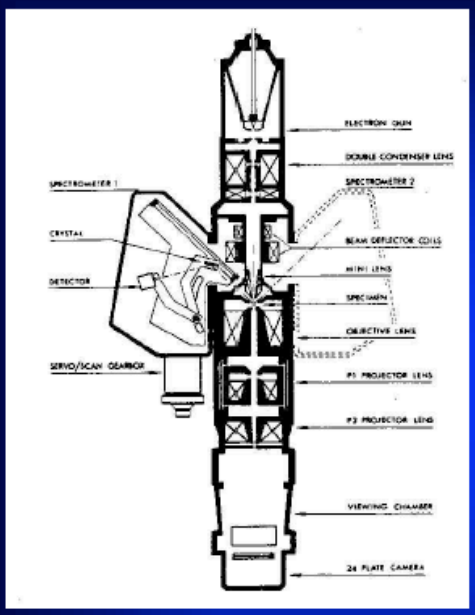

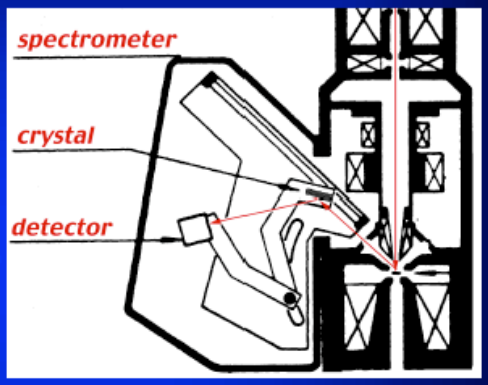

Installation of a Crystal Spectrometer in a TEM - EMMA-4 System

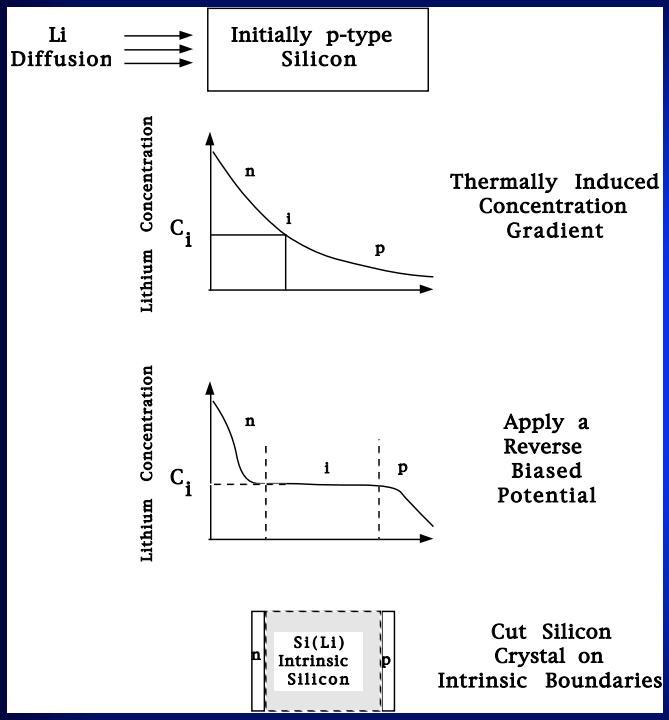

•P-type Silicon high conductivity due to impurities (usually Boron); Lithium acts as a compensating dopant neutralizing the Si giving it a high resisitivity.

• Radiation deposits energy in the Si(Li) lattice & creates free electron-hole pairs in the crystal @ 1 electron-hole pair/3.8 eV of deposited energy @ 77K.

• Intrinsic semiconducting Si allows both electrons & holes to become mobile under application of a potential bias across the crystal

Properties of Intrinsic Silicon

.

Attaching HV electrodes to the two surfaces the Si(Li) crystal will act similiar to a capacitor with free charges developing on the electrical contacts. Charge developed in the crystal is N = E/ε. (E= x-ray Energy, ε = 3.8 eV/e-h pair) i.e. ==> 10 kV X-ray produces ~2630 electrons = 4.2 x 10 -16 Coulombs.

Solid State Detector Construction

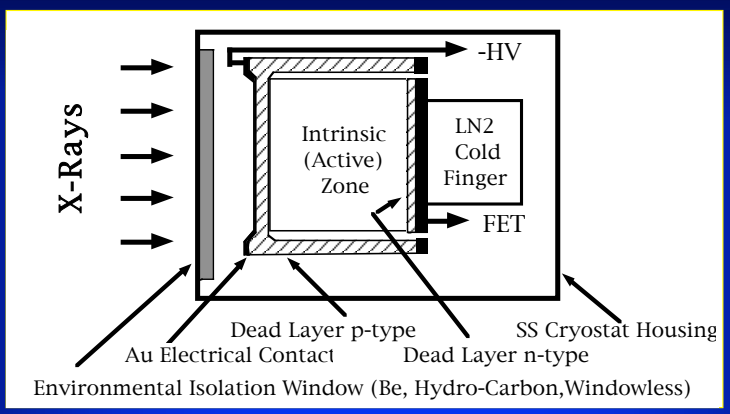

Relative Detection Efficiency

Solid State Detectors: Si(Li) or Instrinsic (High Purity) Ge

Using a simple absorption model define the relative detector efficiency ε(E) by the following procedure:

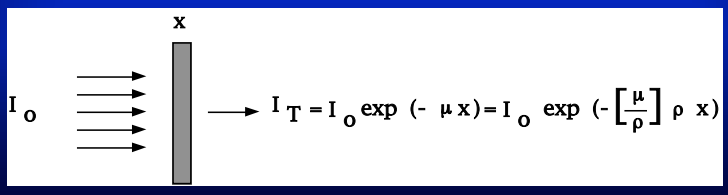

Fabrication of Si(Li) Crystals

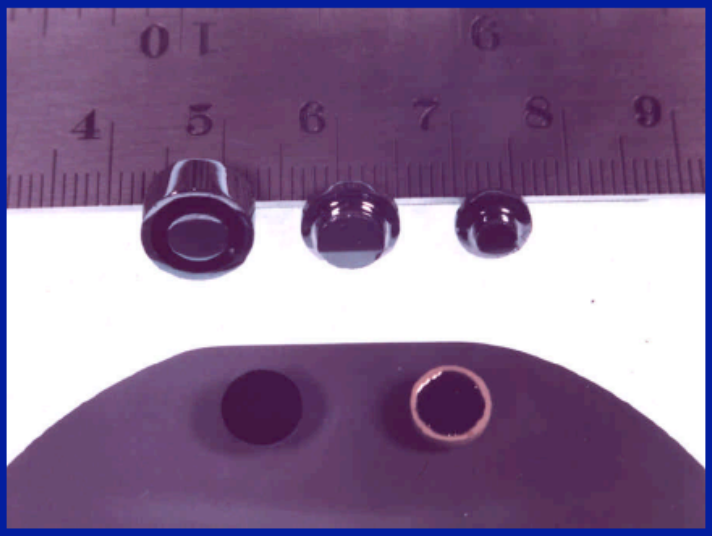

Solid State Detector Construction

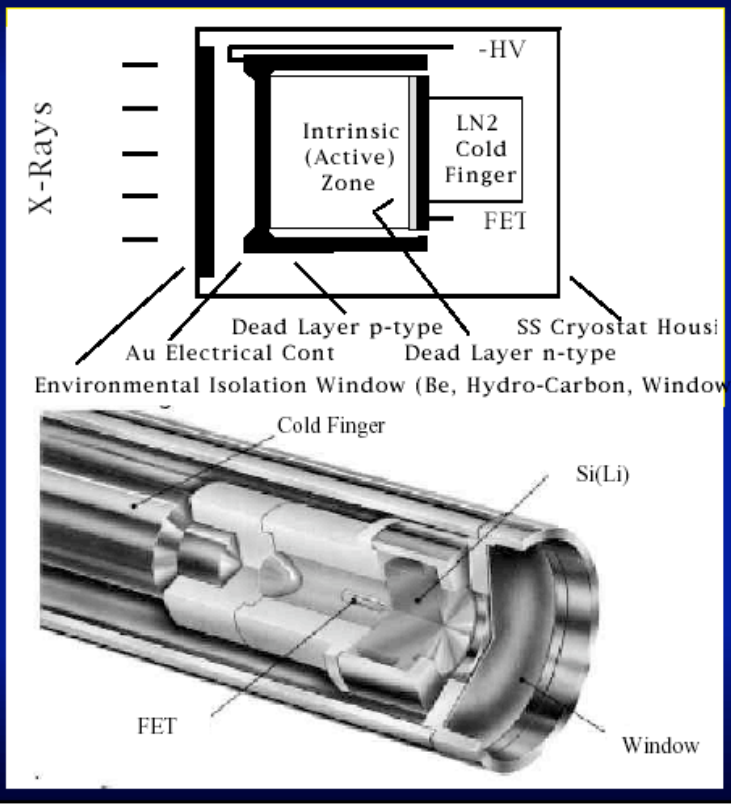

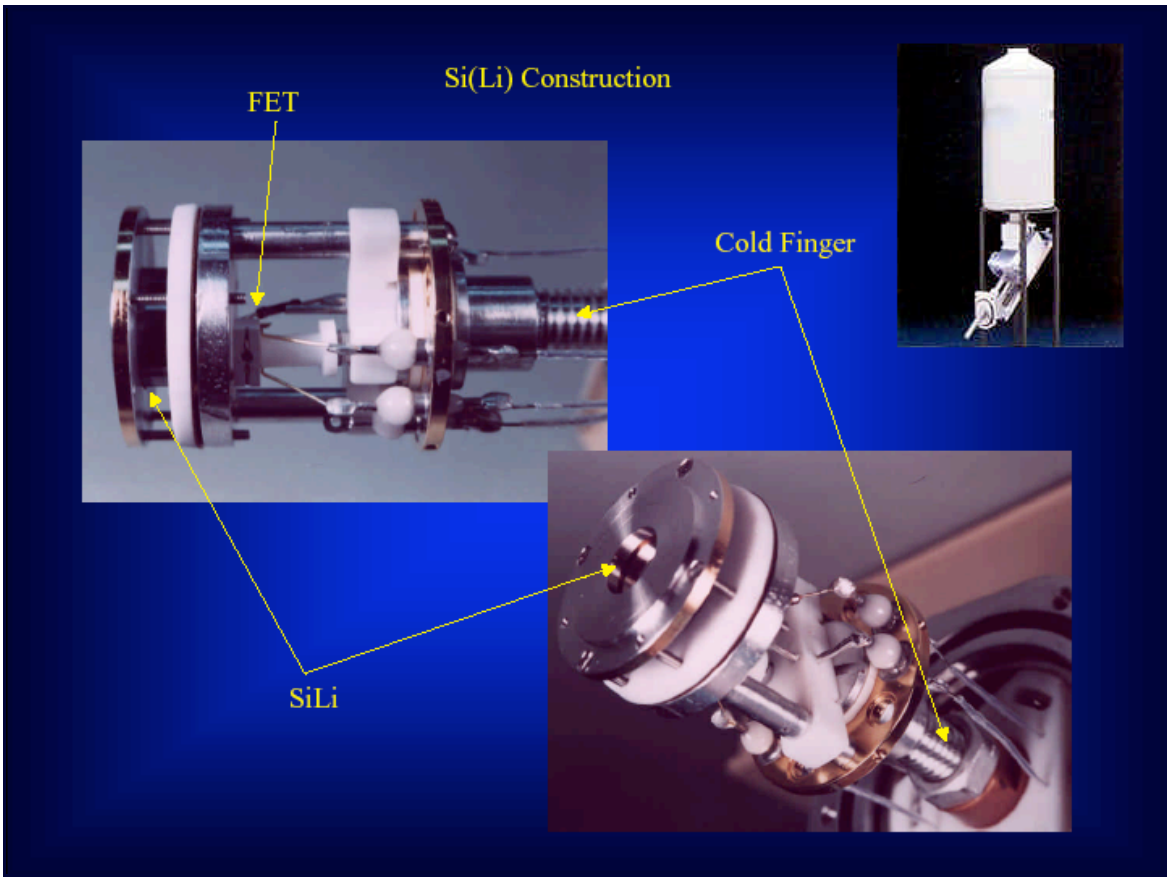
Si(Li) Construction
FET
Cold Finger
SiLi

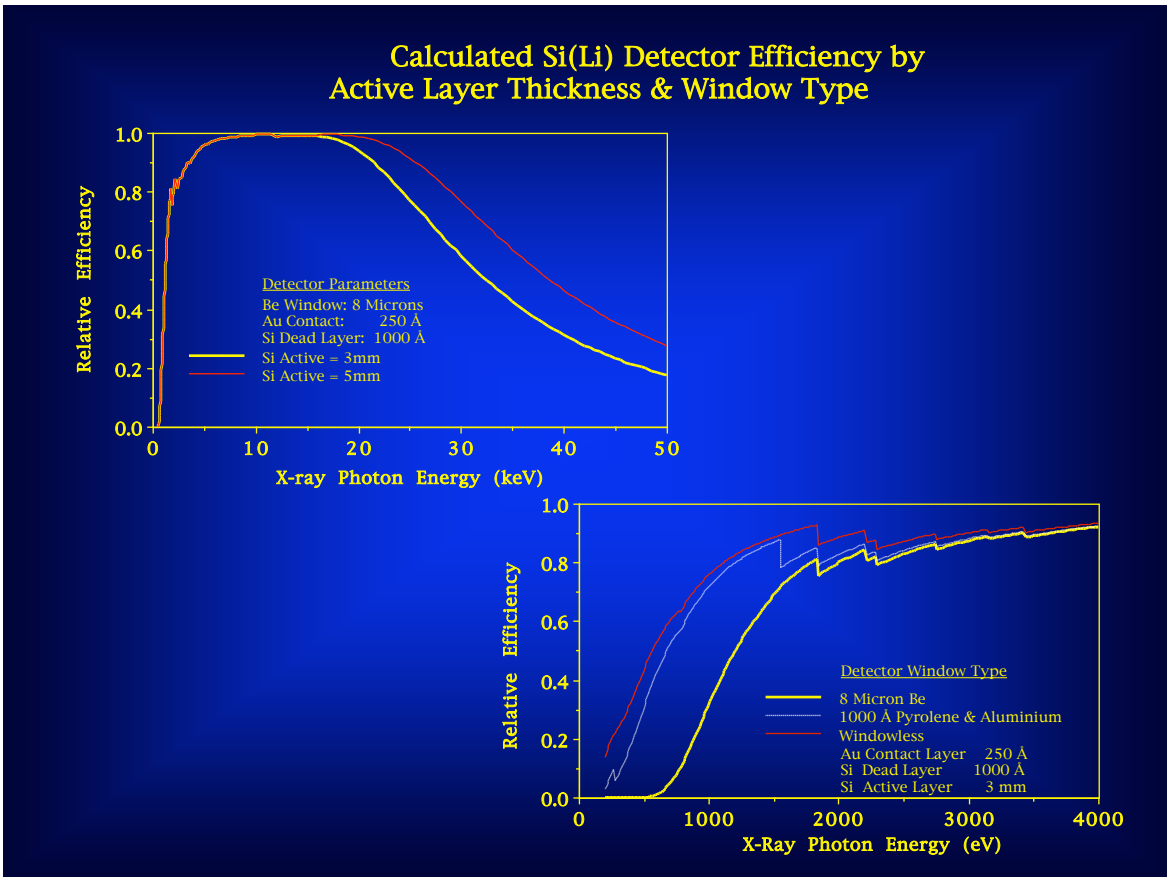
Calculated Si(Li) Detector Efficiency by
Active Layer Thickness & Window Type
Relative Efficiency
1.0
0.8
0.6
0.4
0.2
0.0
0
10
20
30
40
50
X-ray Photon Energy (keV)
Detector Parameters
Be Window: 8 Microns
Au Contact: 250 Å
Si Dead Layer: 1000 Å
Si Active = 3mm
Si Active = 5mm
Relative Efficiency
1.0
0.8
0.6
0.4
0.2
0.0
0
1000
2000
3000
4000
X-Ray Photon Energy (eV)
Detector Window Type
8 Micron Be
1000 Å Pyrolene & Aluminium
Windowless
Au Contact Layer 250 Å
Si Dead Layer 1000 Å
Si Active Layer 3 mm

Relative Transmission Efficiency

$$\varepsilon(E) = \frac{I_T}{I_o} = \exp\left(\sum_{i}^{Window} -\left(\frac{\mu(E)}{\rho}\right)_i * \rho_i * t_i \right)$$

$\frac{\mu(E)}{\rho}$ = mass absorption coefficient for Energy E; ρ = density; t = layer thickness

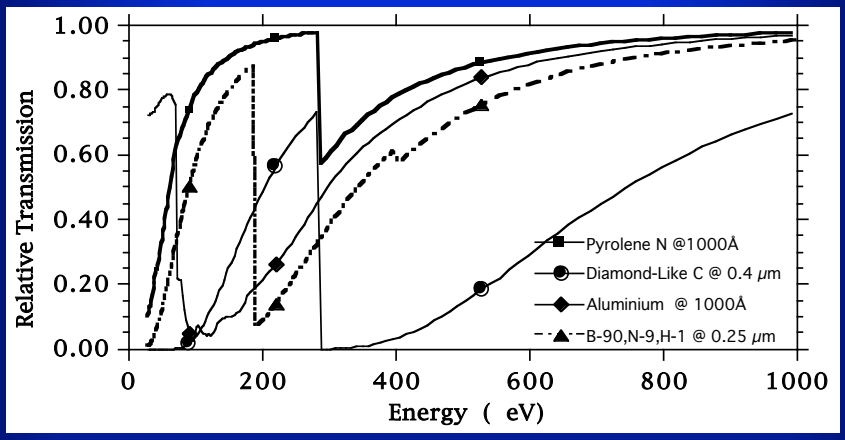

Note the Variation in transmission characteristics by Window Type.
Not all UltraThin Windows are Equivalent!!! For example Detection of Nitrogen using a Diamond window is virtually impossible.

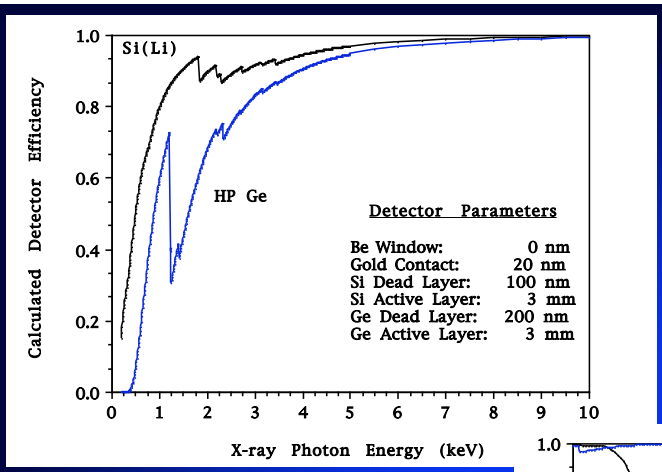

Calculated Efficiency Si(Li) and HPGe Windowless Systems

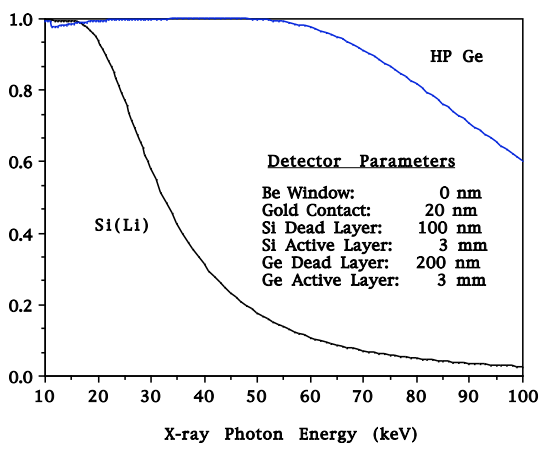

Windowless vs. Conventional Detectors
Comparision of XEDS measurement on NiO using a Windowless versus Beryllium Window detector

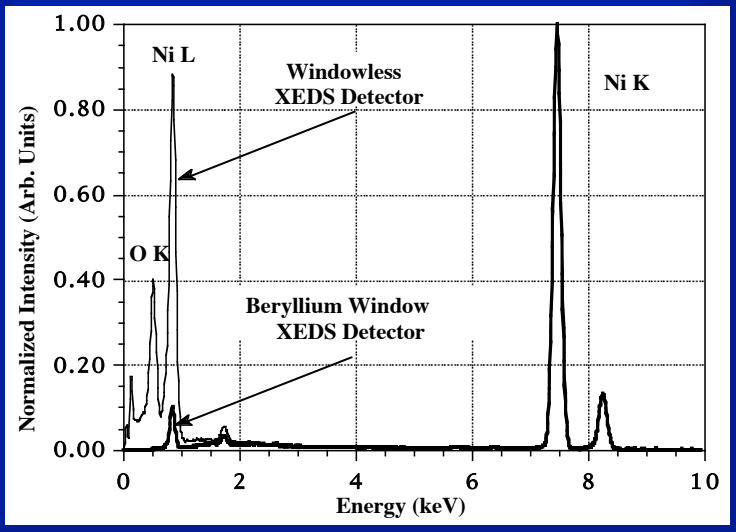

Note the enhanced detection efficiency below 1 keV for the WL detector. Both spectra are normalized to unity at the Ni Kα Line (7.48 keV)

Windowlessvs. Conventional Detectors

K Shell Spectra using Windowless Detector

Boron -> Silicon

L Shell Spectra Using Windowless Detector

Titanium ->Zinc

Note Potential Overlaps with K shell Lines

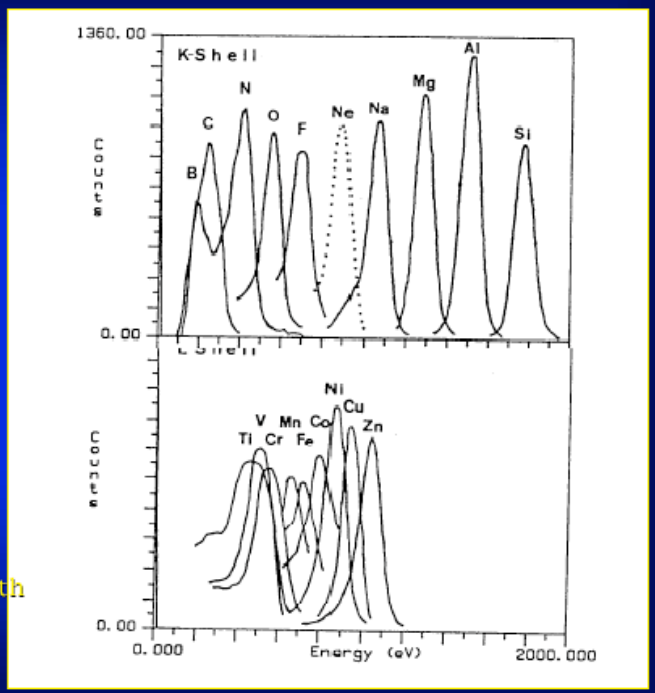

Comparision
Light Element
Spectroscopy
Resolution
XEDS

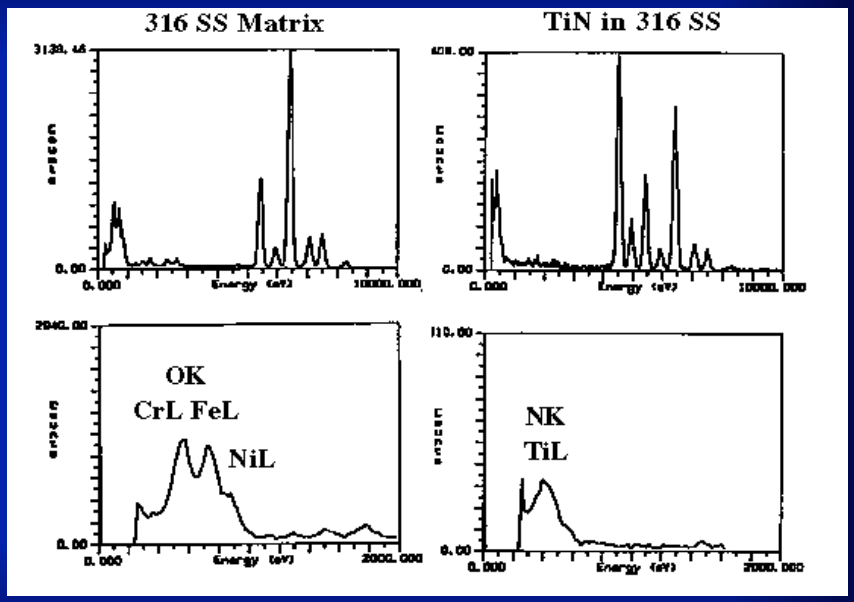

The Multi-Channel Analyzer

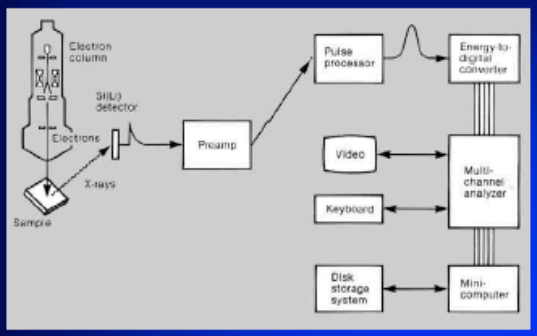

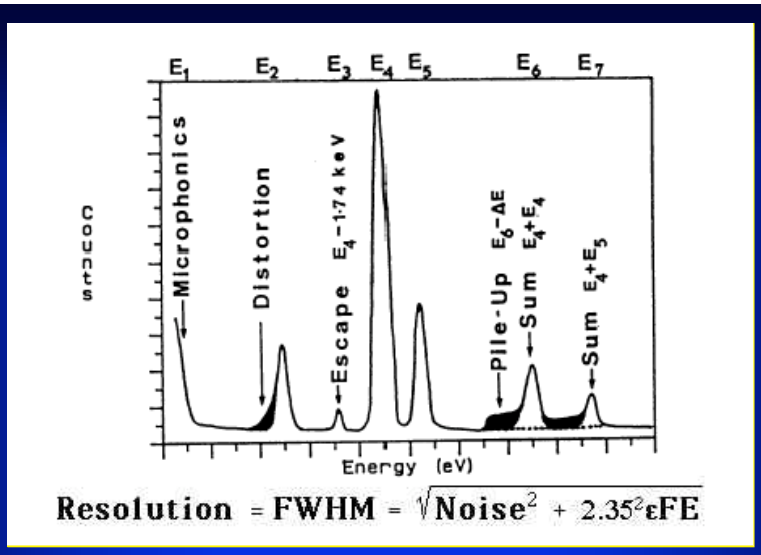

ε= 3.8 eV (in Si) / 2.9 eV (in Ge)
F = Fano Factor ~ 0.1
E= X-ray Energy
Noise = Electronic Noise (mainly in the FET)

Nominal FWHM Values in Modern Si(Li) Detectors:

O Kα (0.52 keV)	= 80 to 100 eV
Mn Kα (5.9 keV)	= 140 to 160 eV
Mo Kα (17.5 keV)	= 210 to 230 eV

Resolution will also vary with Microphonic & Electronic Noise, and Counting Rate!

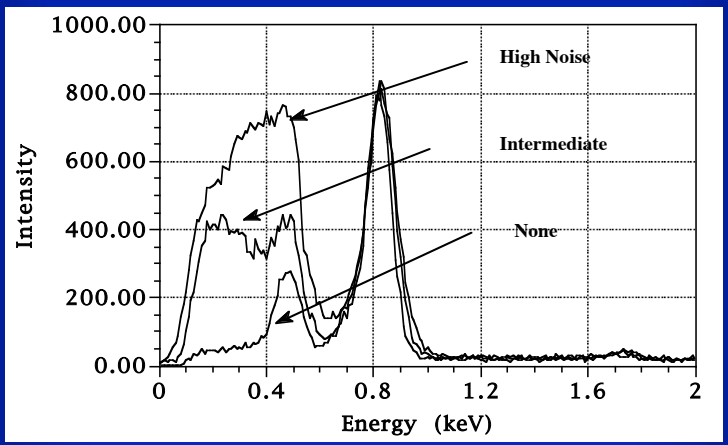

WL & UTW detectors are particularly sensitive to low energy noise and microphonics. Observe the changes in the spectra

Resolution Loss with Count Rate

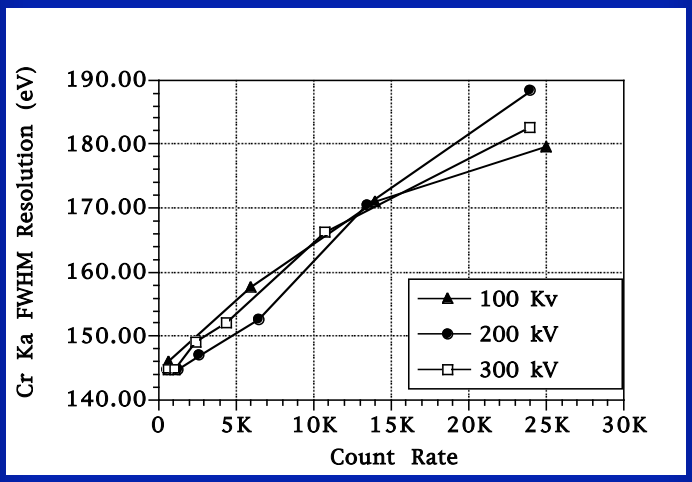

MCA/ADC Considerations
Detector Dead Time

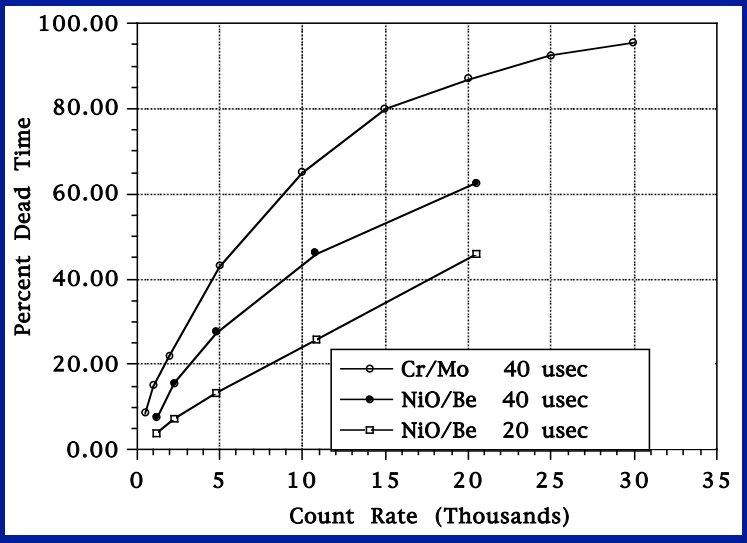

Instrumentation: AEM Systems

The AEM as a system
Spectral Artifacts in the AEM
- Uncollimated Radiation
- Systems Peaks
- Artifacts at High Electron Energy

Specimen Contamination & Preparation
Optimizing Experimental Conditions

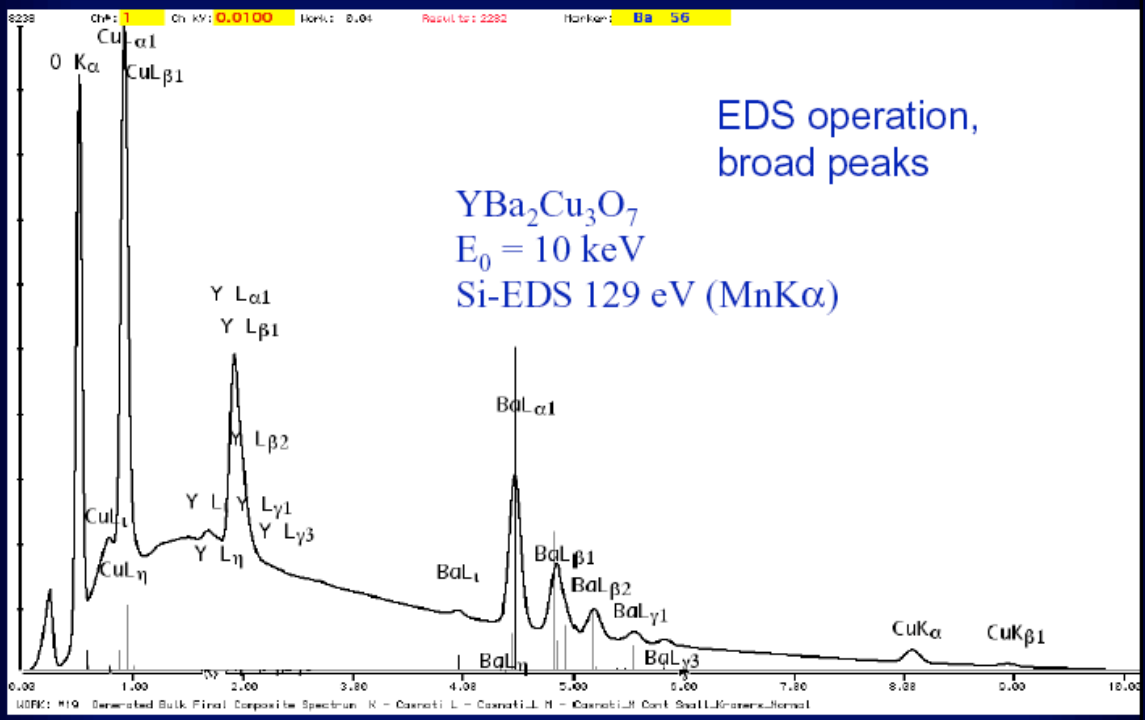

Courtesy of D. Newbury

NIST - Microcalorimetry Approach to EDS

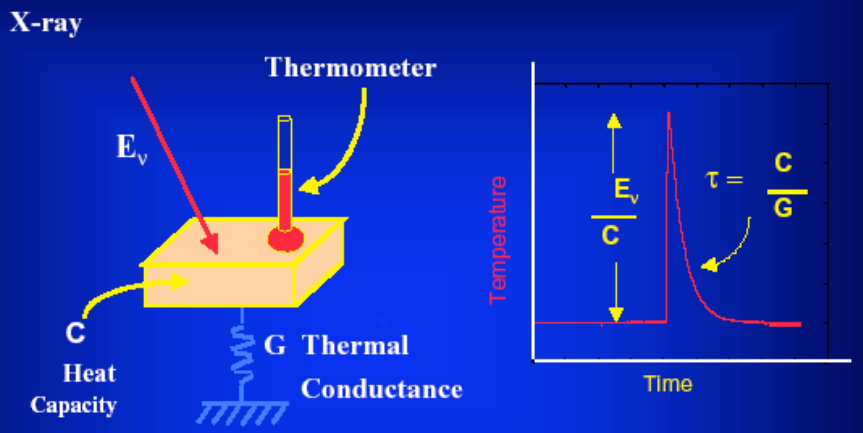

$\Delta E_{FWHM} = 2.36\sqrt{kT^2C}$

Need heat capacity C to be small:

1. Low temperature of operation
2. Small absorber volume
3. Insulators and superconductors

For area ~ mm², thickness ~ few μm
ΔE_{FWHM} ~ few eV at T = 100 mK

NIST Microcalorimeter X-ray Spectrometer

Cryoelectronics schematic

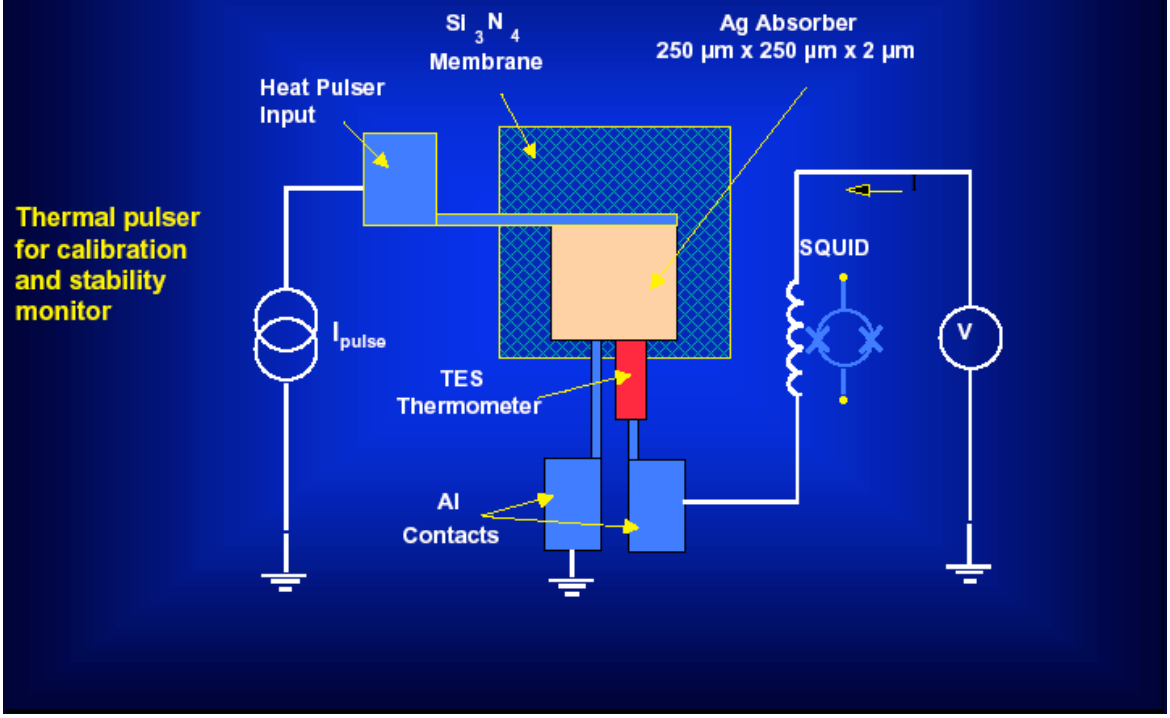

Construction of the cryostat for NIST μcal EDS

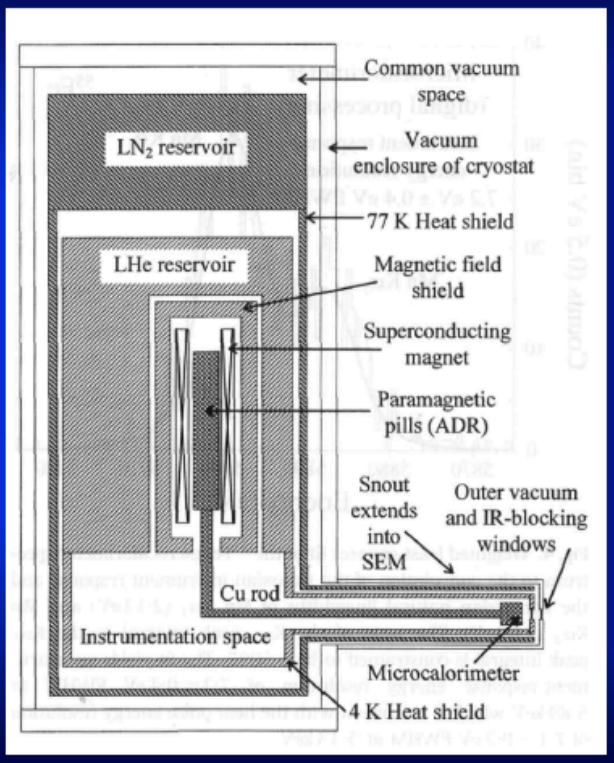

Conventional Si(Li) EDS

NIST Microcalorimeter Cryostat

1. Liquid N_2 to 77K
2. Liquid He to 4 K
3. Adiabatic demagnetization refrigerator to 100 mK

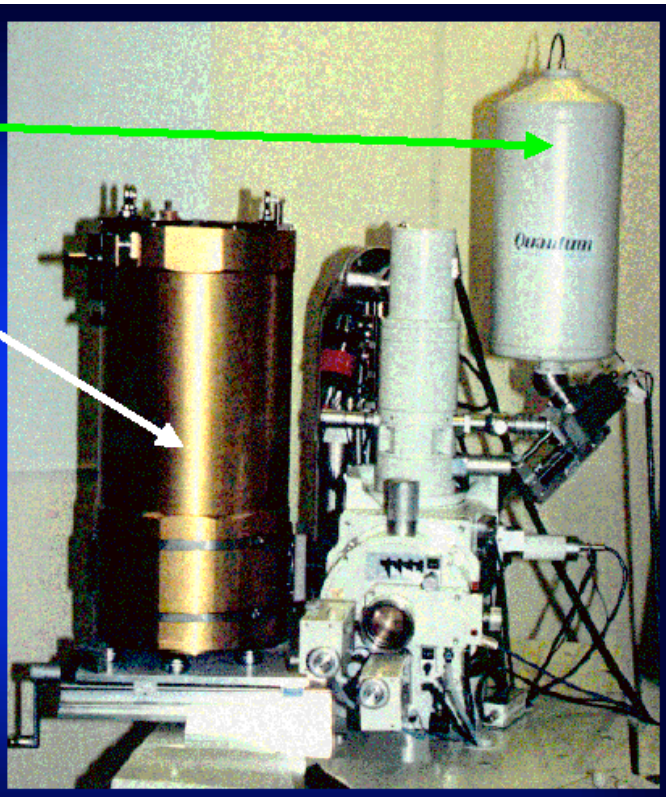

NIST Microcalorimeter X-ray Spectrometer

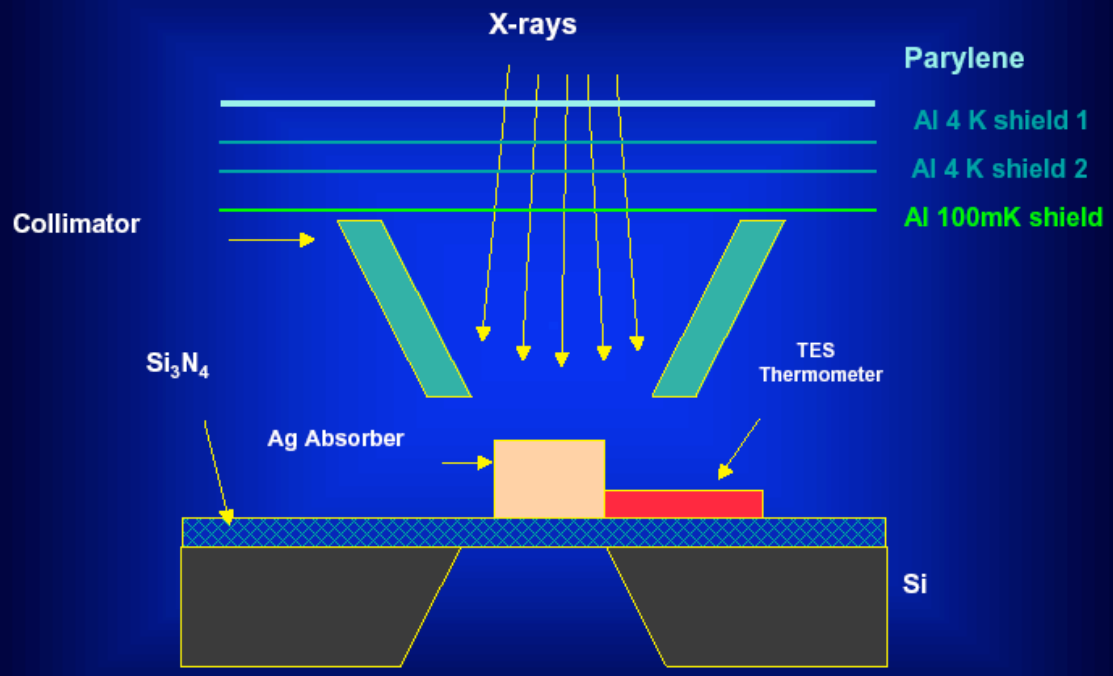

Spectral Artifacts in the AEM
Uncollimated Radiation: The Hole Count

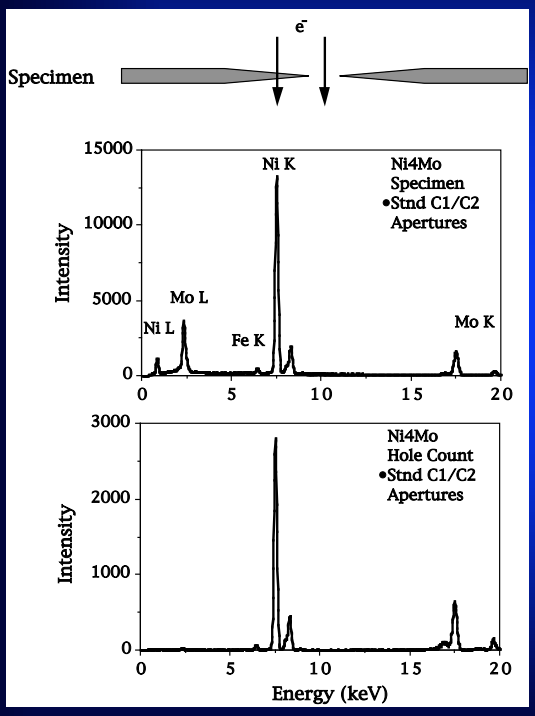

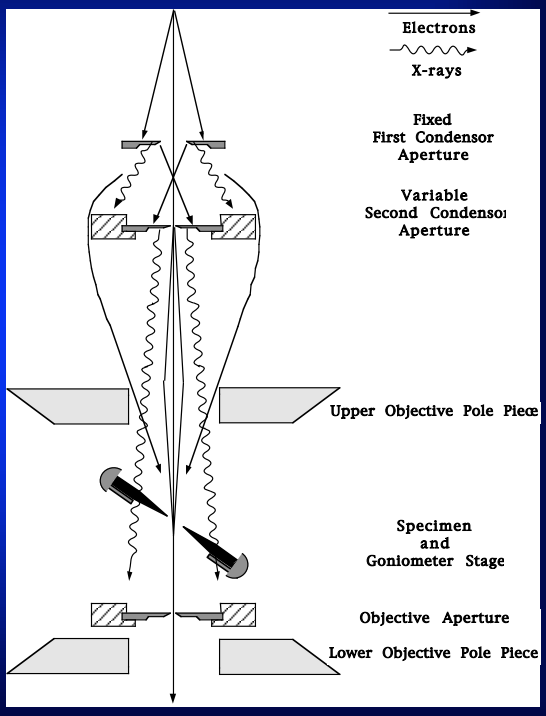

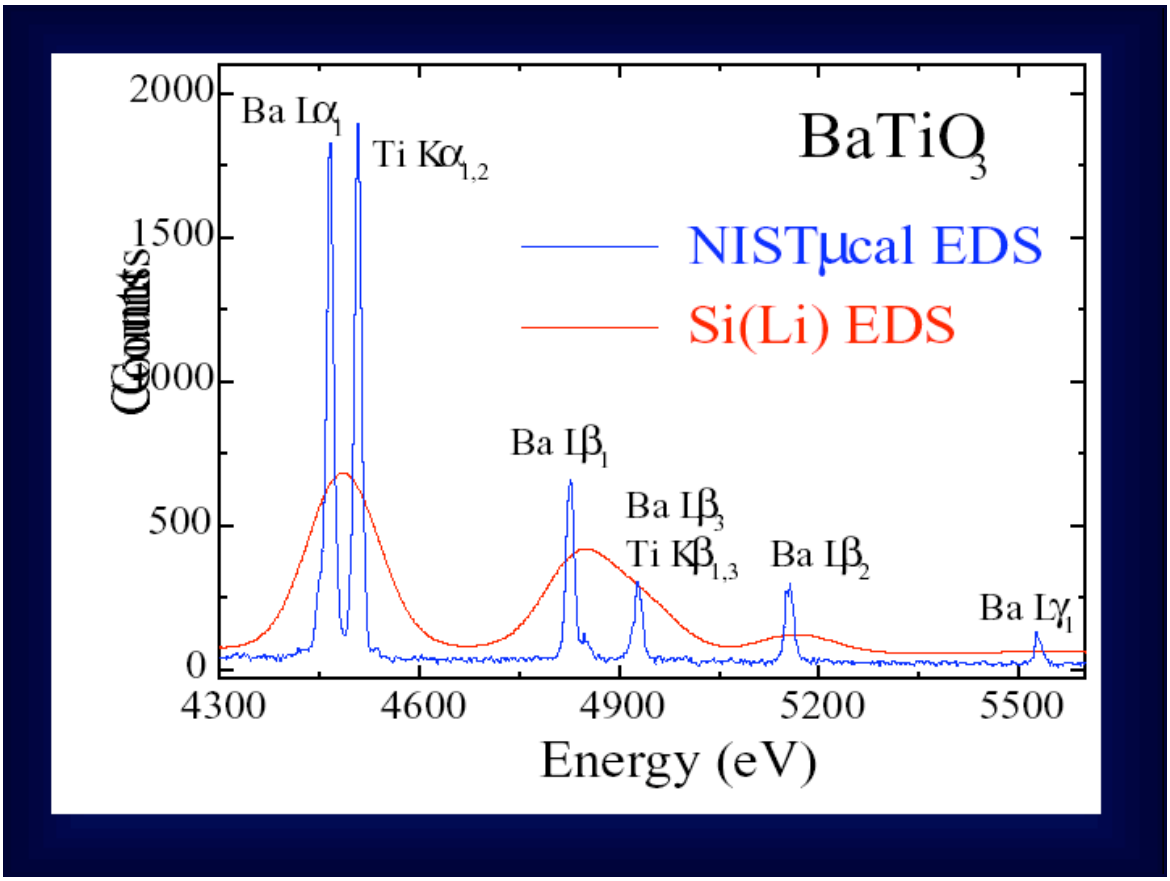

Solid angle limitations

Detector 0.5x0.5 mm at 37 mm
$\Omega = A/r^2 =$ 0.00018 sr

Obviously, This is a very small solid angle detector!

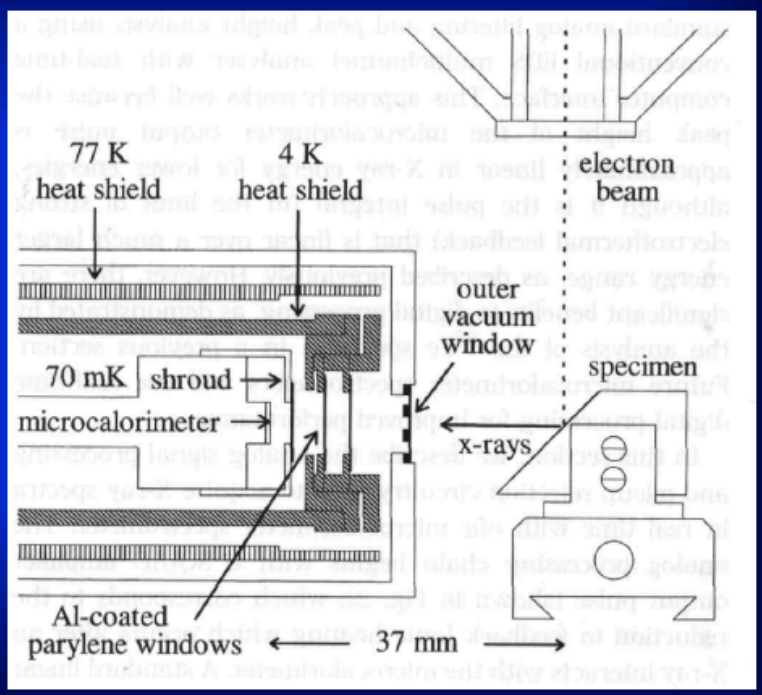

Energy Resolution

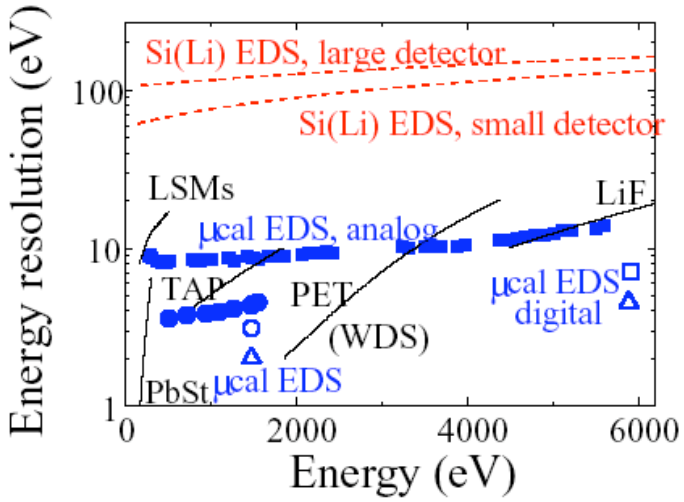

Low Photon Energy NIST Microcalorimeter

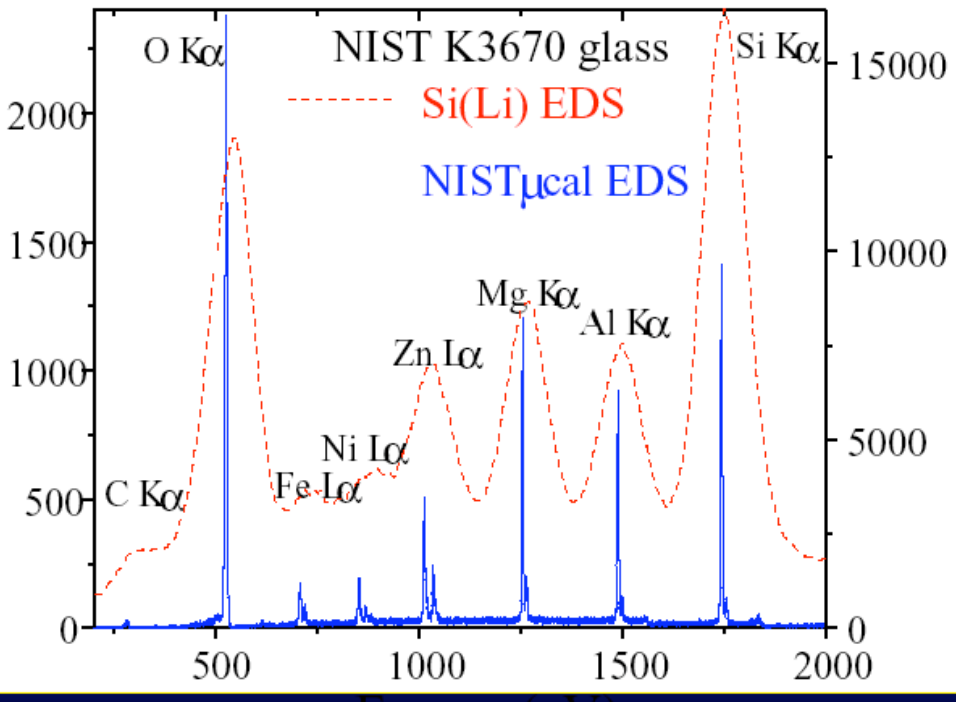

Courtesy of D. Newbury

Spectral Artifacts in the AEM
Uncollimated Radiation Solutions

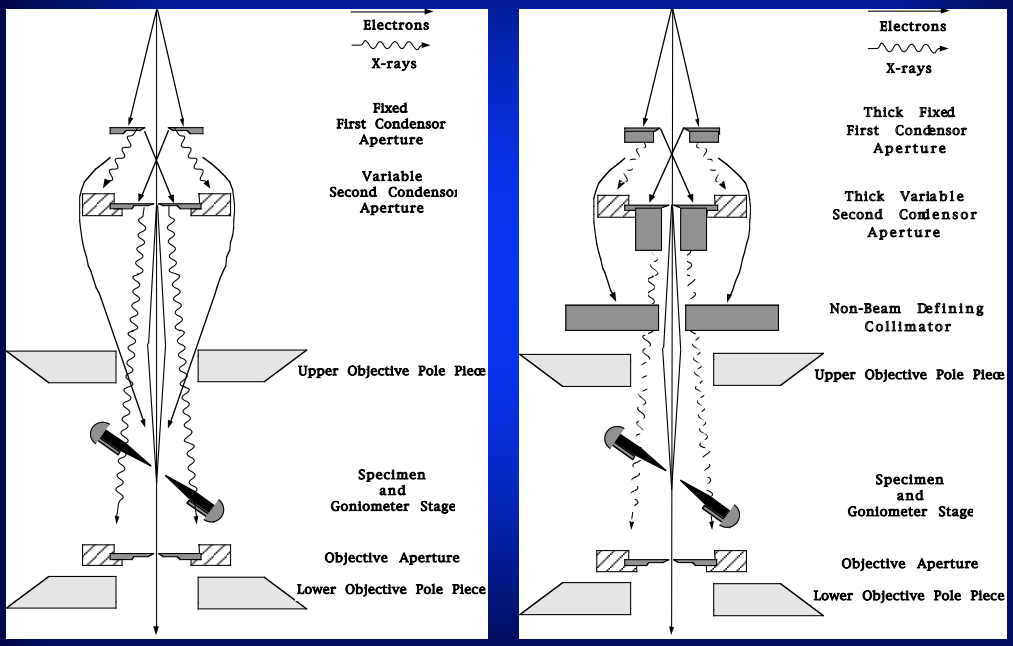

Uncollimated Radiation: The Hole Count
Effects of Thickness & Composition of Variable C2 Aperture

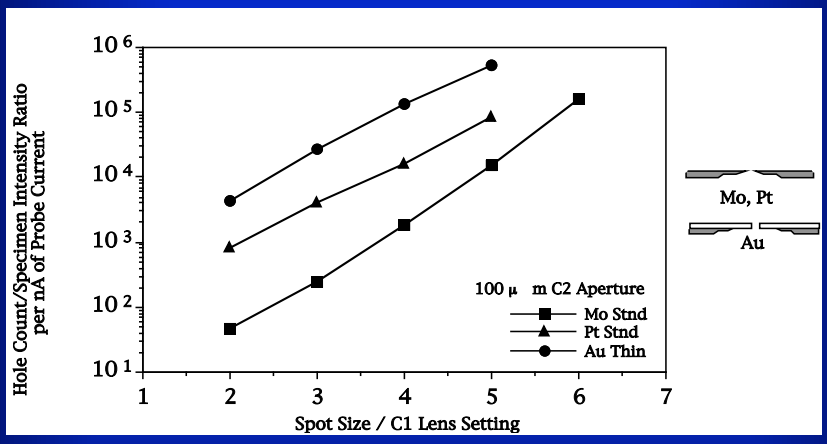

Spectral Artifacts in the AEM

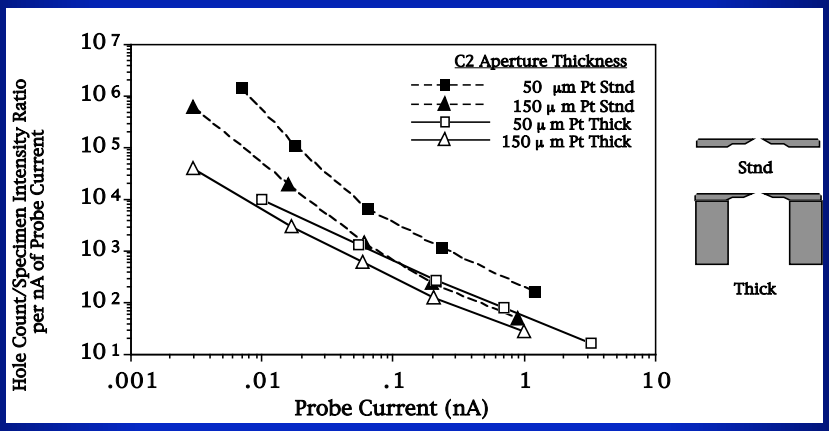

Specimen: 200 Å Molybdenum Film on Holey Carbon supported on a Stnd Mo Aperture with 200 µm hole. Expt. Conditions: 120 kV, Specimen tilted toward Si(Li) 35 degrees.

Spectral Artifacts in the AEM

Hole Count Effects: Modified C_1 and C_2 Apertures

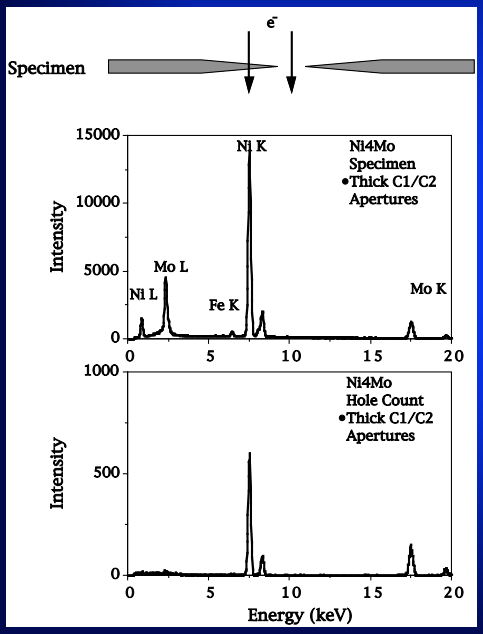

Hole Count Effects: Modified C_1 and C_2 & Non-Beam Defining Apertures

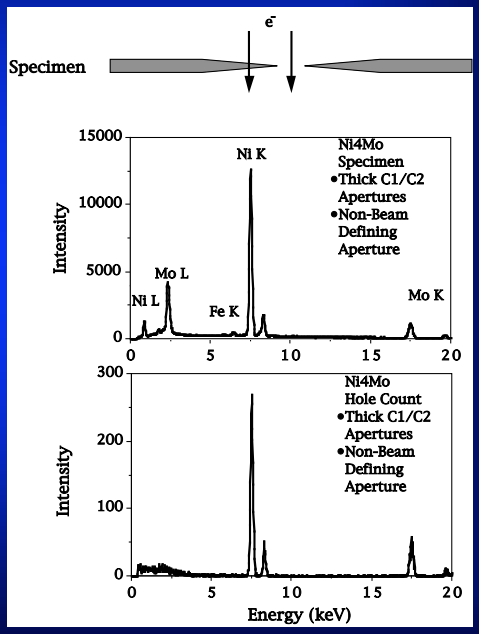

AEM/XEDS Hole Count Test Specimen

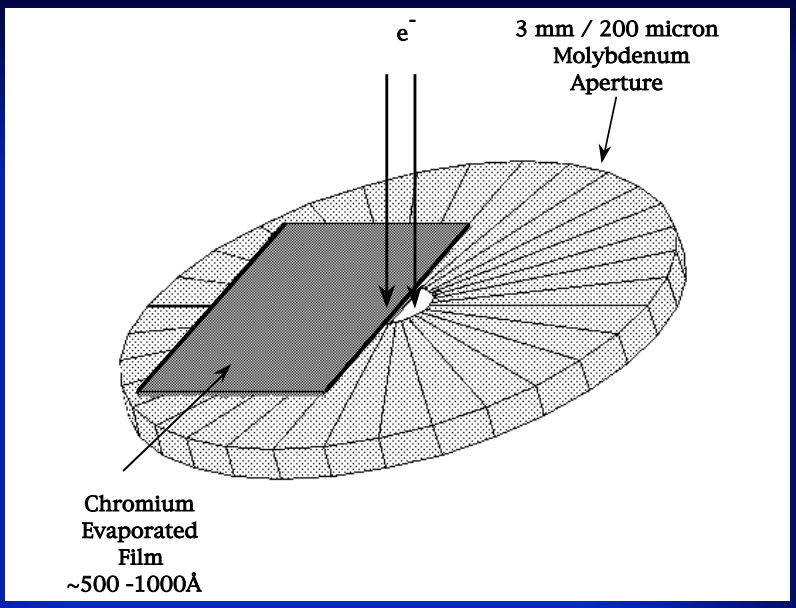

1989 Higgs Meeting XEDS/AEM Performance Panel Members

Bentley -Oak Ridge Nat. Lab
Cazaux - UFR Sciences
Craven - Univ. of Glasgow
Glas-Lab. de Bagneux
Hren-NC State Univ.
Kruit-Delft Univ.
Malisl-PMRL/CANMET
Rez-ASU
Williams-Lehigh Univ.
Zaluzec-Argonne Nat. Lab.

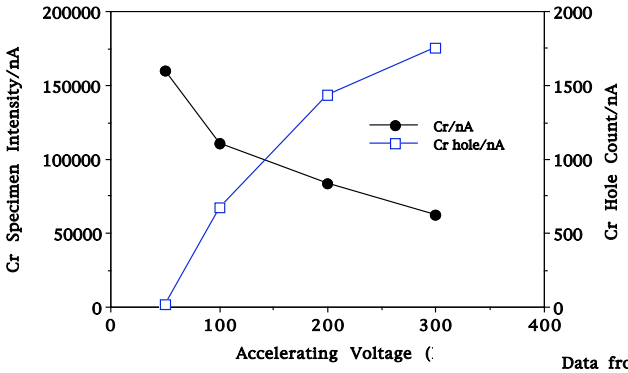

Experimental hole count information available using the AEM/XEDS Cr/Mo test specimen

- Cr and Cr-hole count /nA is used to identify the source of the uncollimated radiation
- Magnitude of the hole count signal is monitored by the ratio of the Mo-hole to Cr specimen intensity

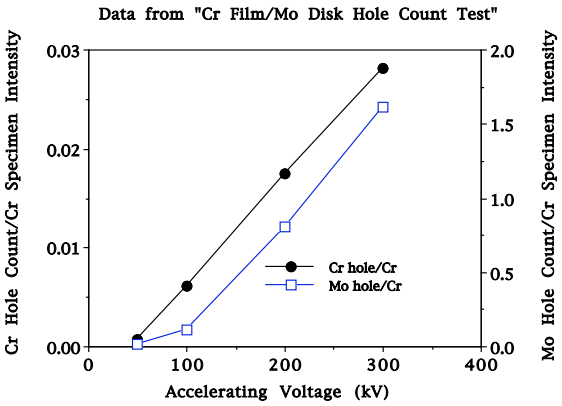

Spectral Artifacts in the AEM: Electrons Entering the Detector 50 kV

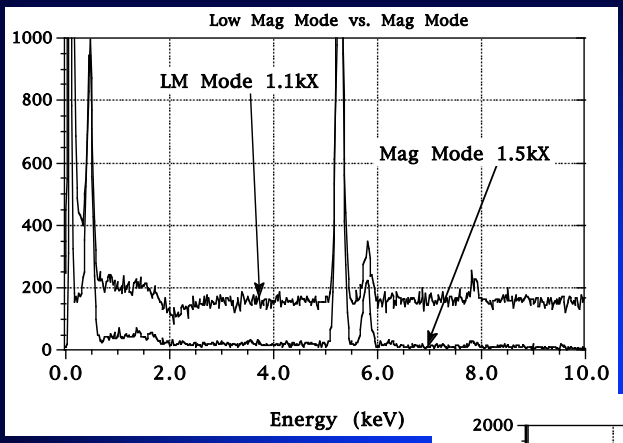

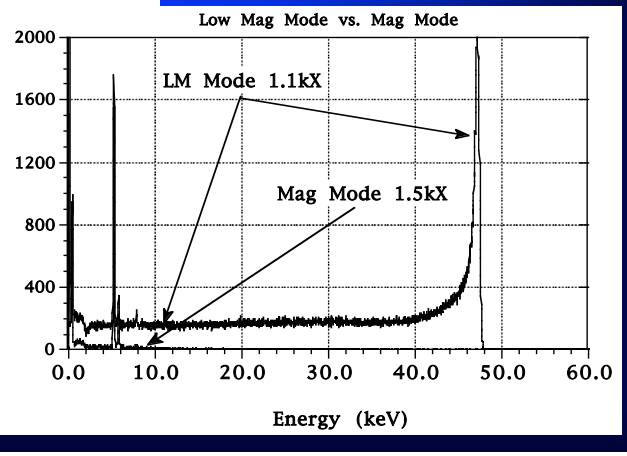

Note the Effects of 50 keV Electrons Entering the Detector on Background

Spectral Artifacts in the AEM: Electrons Entering the Detector 300 kV

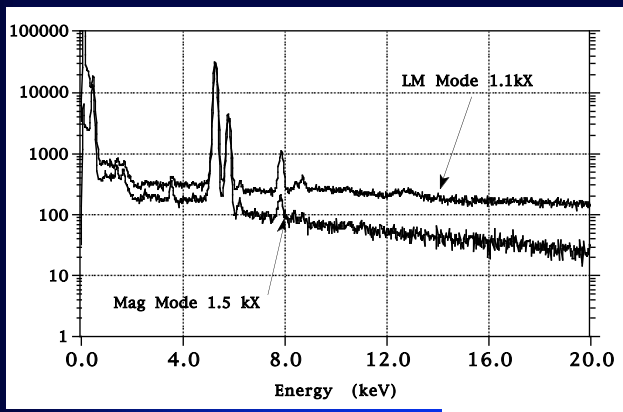

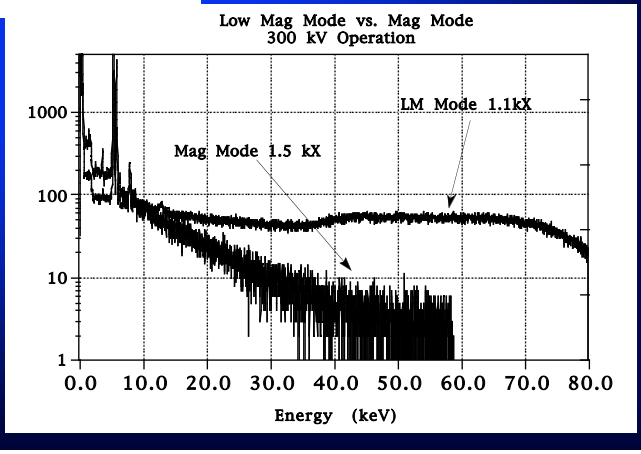

Note the Effects of 300 keV Electrons Entering the Detector on Background

Optimizing Experimental Conditions

Choice of X-ray Line
- K- series
- L- series
- M- series

Detector/Specimen Geometry
- Elevation Angle
- Solid Angle

Detector Collimation

Choice of Accelerating Voltage
- Relative Intensity
- Peak/ Background
- Systems Peaks/Uncollimated Radiation

Choice of Electron Source
- Spatial Resolution
- Tungsten Hairpin
- LaB_6
- Field Emission

Radiative Partition Function (Γ) Governs the Relative Intensities
Nominal Values (Varies slowly with Atomic Number)

K Shell	L Shell	M Shell
$K_{\alpha 1}$ = 100	$L_{\alpha 1}$ = 100	$M_{\alpha 1,2}$ = 100
$K_{\alpha 2}$ = 50	$L_{\alpha 2}$ = 50	M_{β} = 60
$K_{\beta 1}$ = 15-30	$L_{\beta 1}$ = 50	
$K_{\beta 2}$ = 1-10	$L_{\beta 2}$ = 20	
$K_{\beta 3}$ = 6-15	$L_{\beta 3}$ = 1-6	
	$L_{\beta 4}$ = 3-5	
	$L_{\gamma 1}$ = 1-10	
	$L_{\gamma 3}$ = 0.5-2	
	L_{η} = 1	
	L_{ι} = 1-3	

Detector/Specimen Geometry

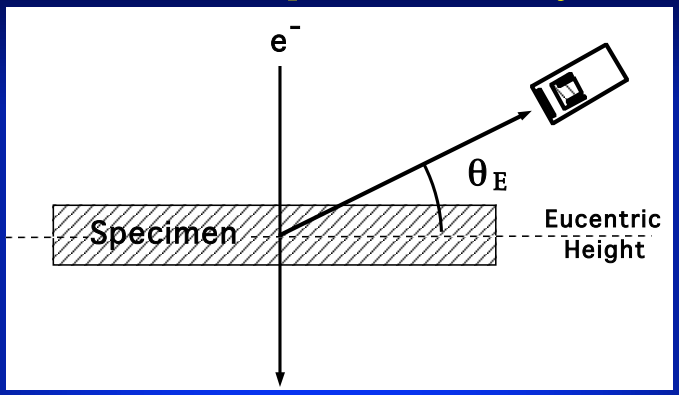

Designation	Elevation Angle θ_E	Azimuthal Angle θ_A	Manufacturer
Low	0° 0°	45° 90°	JEOL JEOL, FEI, VG
Intermediate	15-30°	90°	FEI, JEOL, Hitachi,VG
High	68-72°	0°	Hitachi, JEOL

Detector/Specimen Geometry

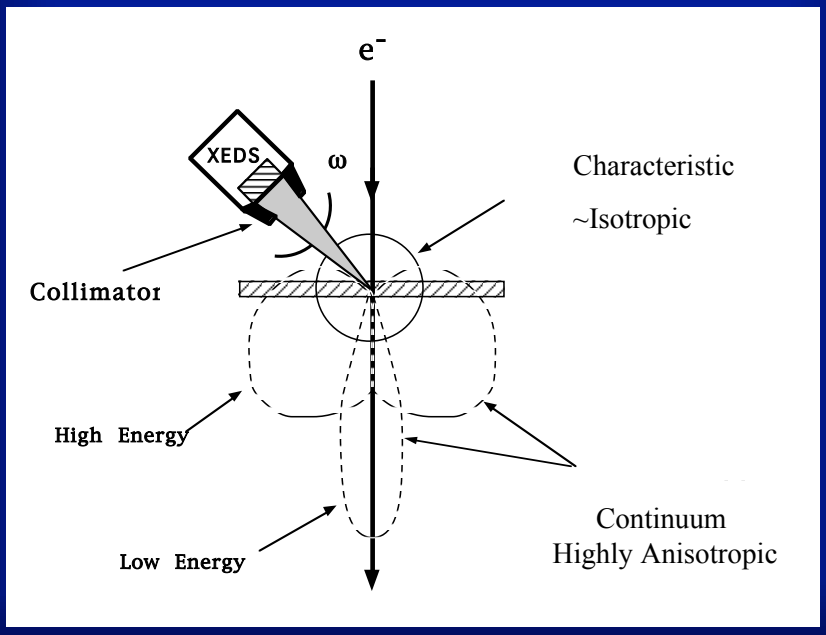

Detector/Specimen Geometry

Collection Solid Angle

$\omega = A/R^2$ = 0.3 - 0.001 sR
A = Detector Active Area
= 10-30 mm2
R = Crystal to Specimen Distance
= 10 - 50 mm

Subtending Solid Angle

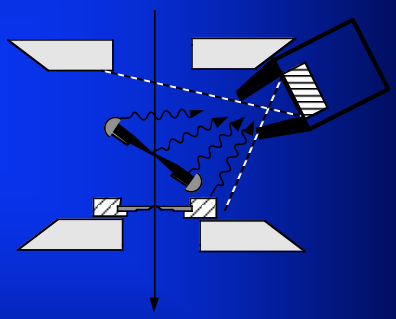

Detection of System Peaks
Effects of the Collimator & Stage

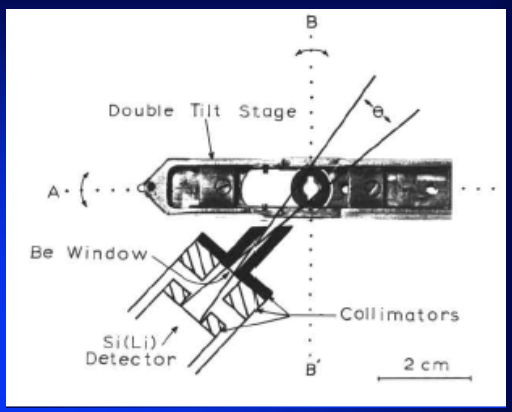

Subtending Solid Angle

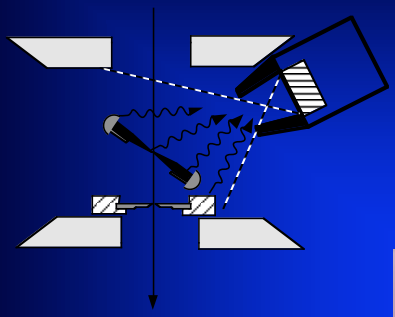

Detection & Removal of System Peaks

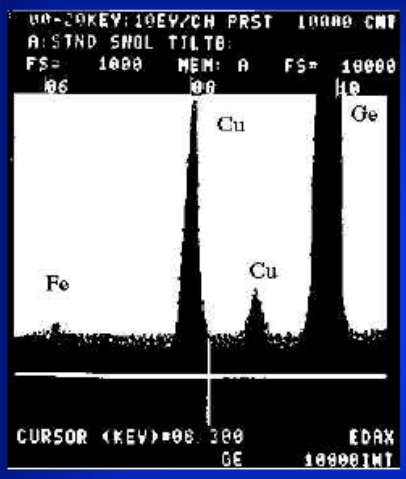

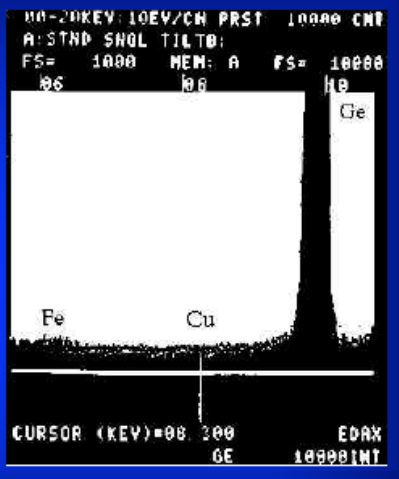

Removal of Stage System Peaks by use of Beryllium Gimbals
Ge specimen 10,000 in Ge Kα peak in both spectra
Left Standard Single Tilt Cu Stage, Right Be Gimbal DT Stage

Reactive Gas Plasma Processing Applications to Analytical Electron Microscopy

Example:

- The figure at the right shows the results of contamination formed when a 300 kV probe is focussed on the surface of a freshly electropolished 304 SS TEM specimen.

- The dark deposits mainly consist of hydrocarbons which diffuse across the surface of the specimen to the immediate vicinity of the electron probe. The amount of the contamination is a function of the time spent at each location. Here the time was varied from 15 - 300 seconds.

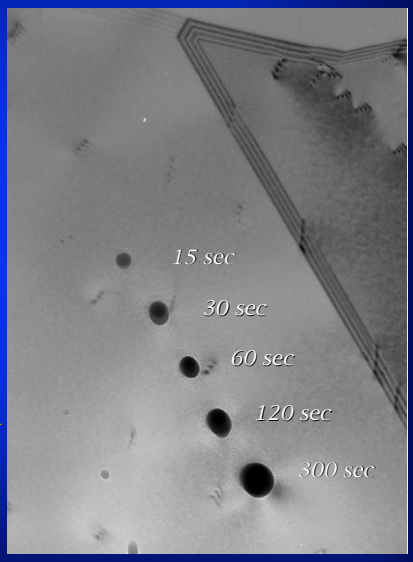

Comparision Results on Electropolished 304 SS

- Untreated Specimen
- After 5 minutes Argon Processing
- After 5 minutes of additional Oxygen Processing

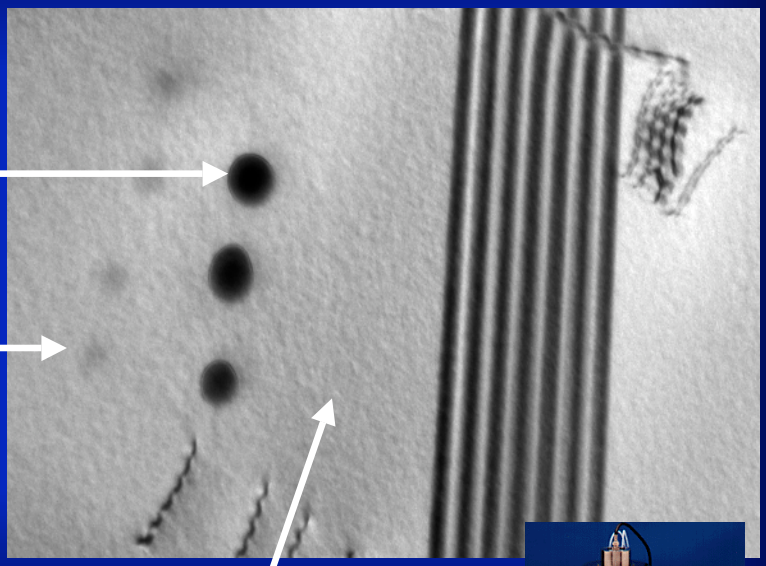

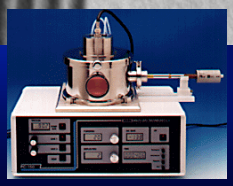

Maximizing The Signal

X-ray Production = Cross-section * electrons

η = Probe current = $\frac{(\pi d_o \alpha_o)^2 \mathcal{B}}{4}$

$\mathcal{B}$ = Brightness = $(\frac{J_c}{\pi kT}) eV_r$

V_r = Relativistic Voltage = $V_o(1+\frac{eV_o}{[\ 2m_oc^2\ ]})$

$V_o(\ 1+ 9.785 \times 10^{-7} V_o)$

Relativistic Cross-section Model

$$Q_K = \frac{a_K * b_K * \{\ \ln\ (c_K * \frac{T_o}{E_c}) - \ln(1-\beta^2) - \beta^2\}}{T_o * E_c}$$

$T_o = 1/2\ m_oc^2\beta^2$, where $\beta = v/c$

Specimen Contamination Effects

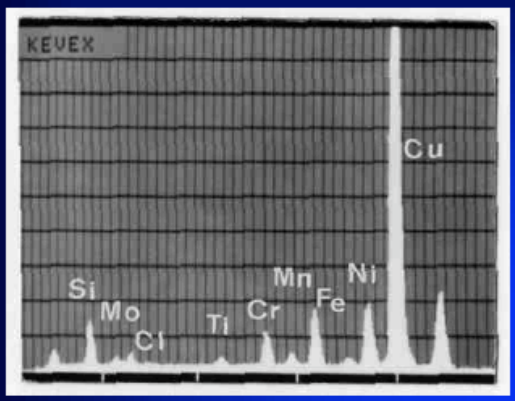

Electropolishing leaves residual Cl on surface

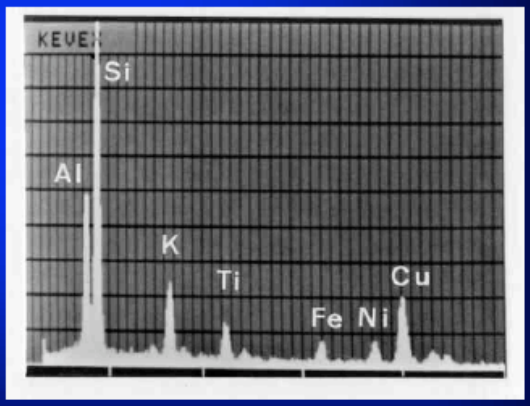

Ion Milling leaves redeposited Fe, Ni, Cu from SS Holder & Cu Washer

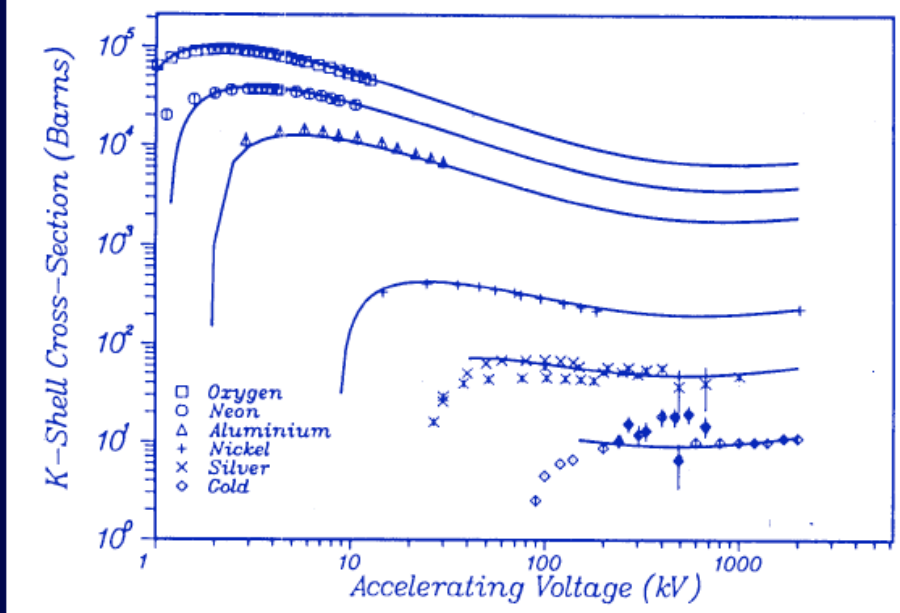

Effects on Intensity with Accelerating Voltage for constant Probe size parameters

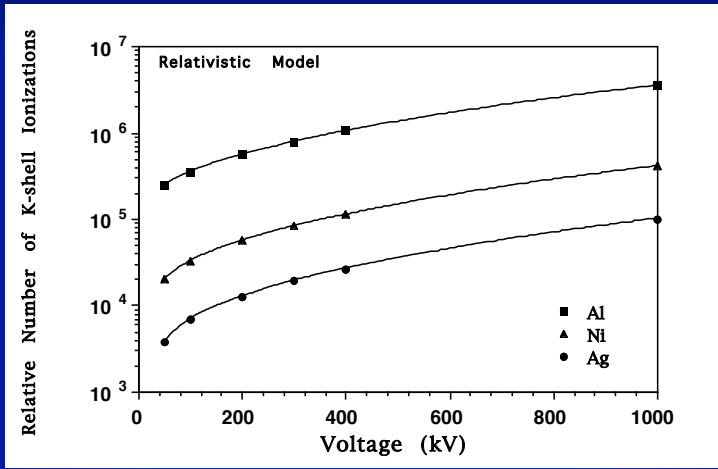

$$I = Q * \eta$$

For identical probe diameters one has higher x-ray production at higher voltage due to the increase in beam current.
Alternatively, one can achieve the same statistical intensity for smaller probes at higher

Experimental Variation of Beam Current and X-ray Intensity with Voltage

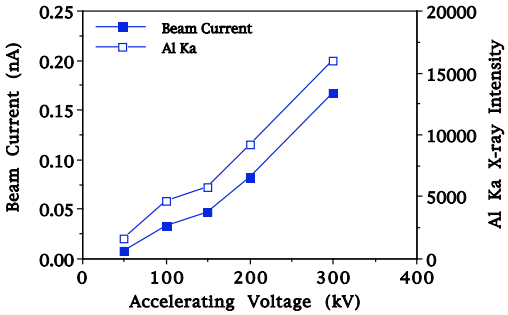

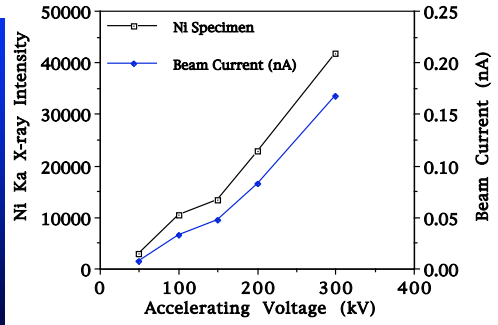

Minimium Detectable Mass

$$MDM \sim \frac{k}{P_x I_o \tau} = \frac{k^*}{P_x J_o d_o^2 \tau}$$

Minimum Mass Fraction

$$MMF \sim \frac{k}{\sqrt{[P_x (\frac{P}{B})_x I_o \tau]}} = \frac{k^*}{\sqrt{[P_x (\frac{P}{B})_x J_o d_o^2 \tau]}}$$

k,k^* = Constants

P_x = Characteristic Signal from element X

$(P/B)_x$ = Peak to Background ratio for element X

I_o = Incident electron flux

J_o = Incident electron current density

d_o = Probe diameter

τ = Analysis time

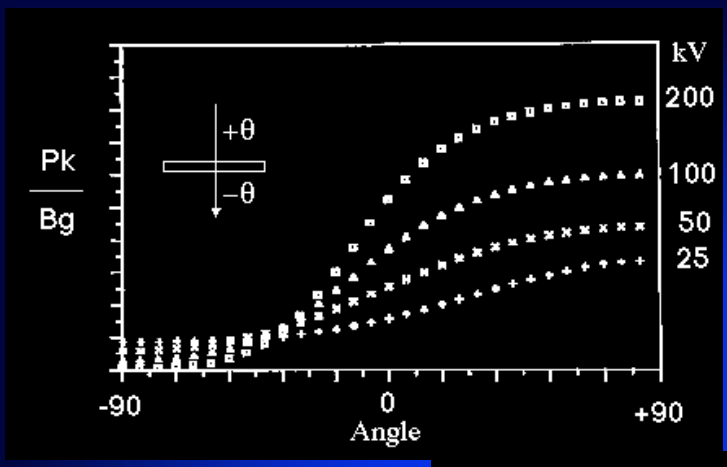

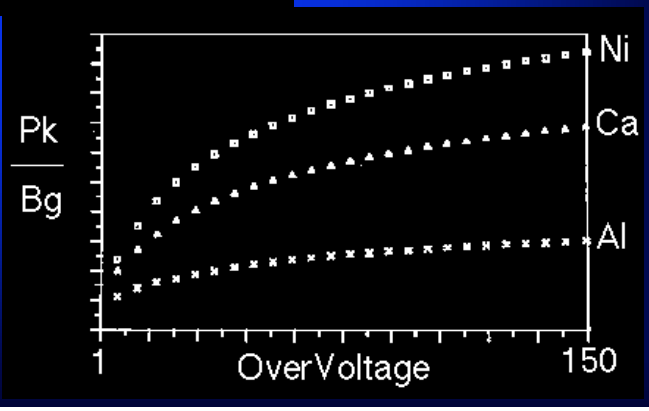

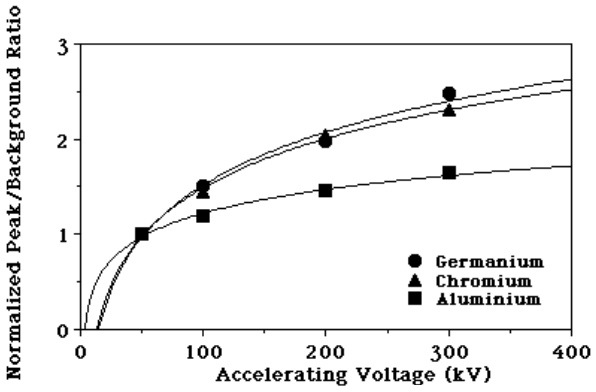

Experimental
Peak/Background
Variation with Voltage

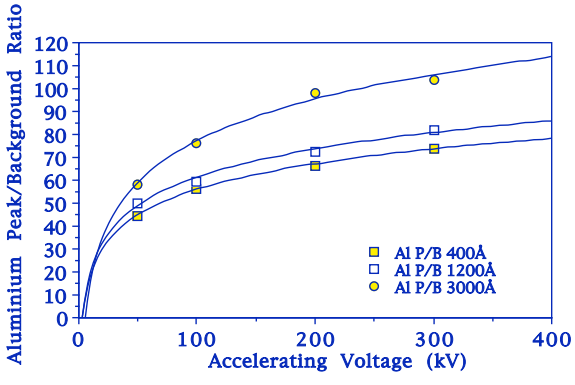

Spatial Resolution /Beam Spreading Monte Carlo Calculations

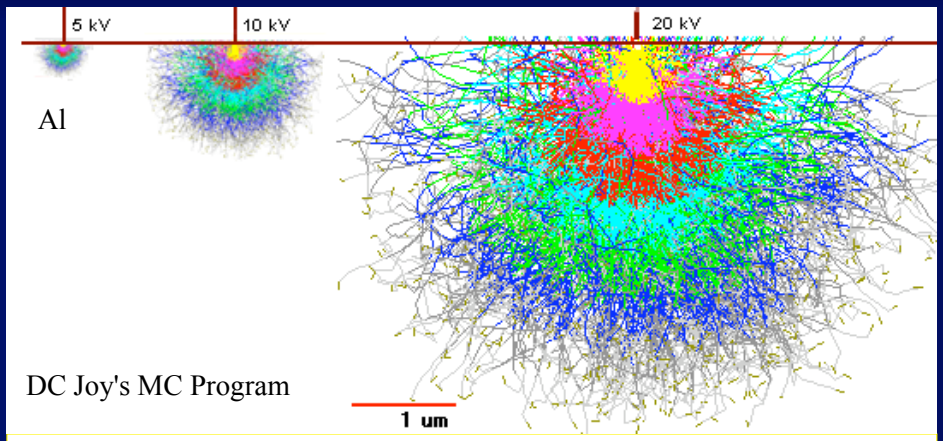

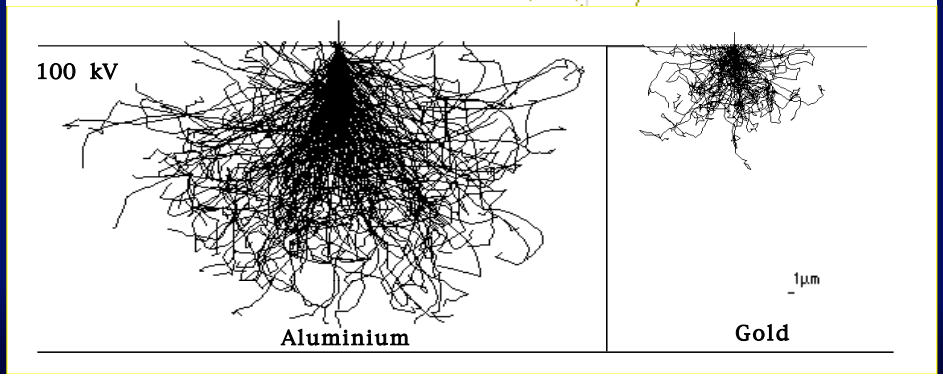

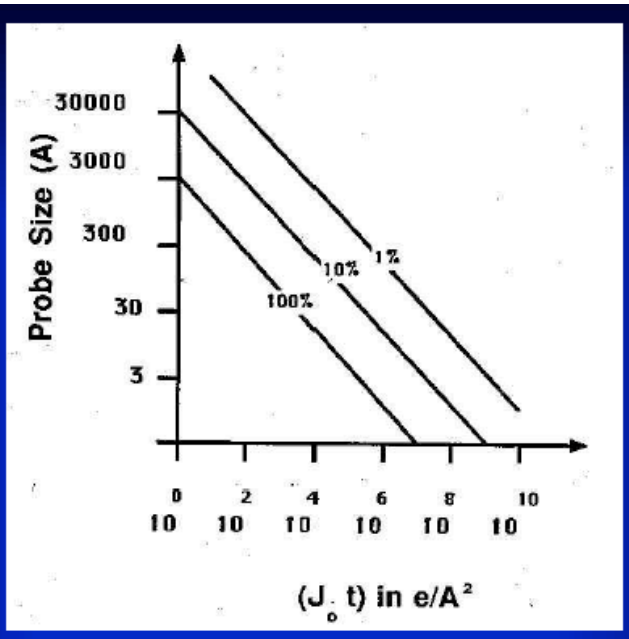

$$d_o = \frac{k}{MMF}\left[\frac{1}{P_x (P/B)_x J_e t}\right]^{1/2}$$

Minimum Detectable Mass

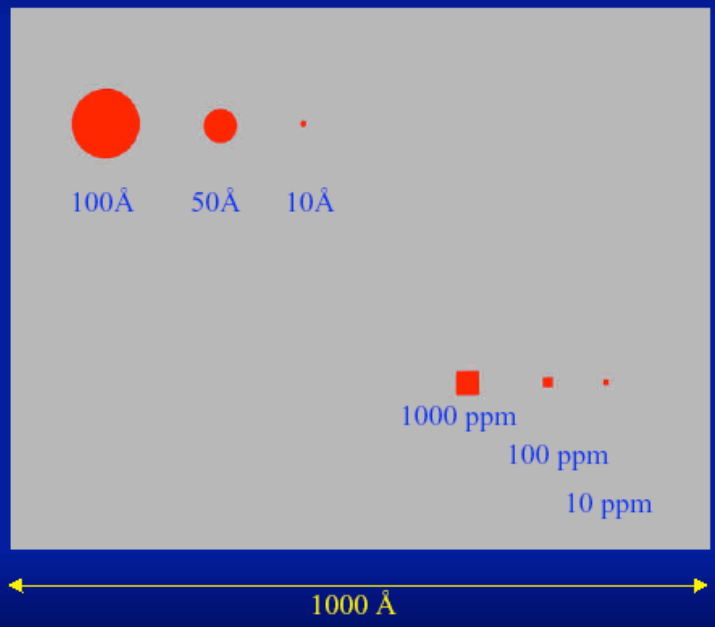

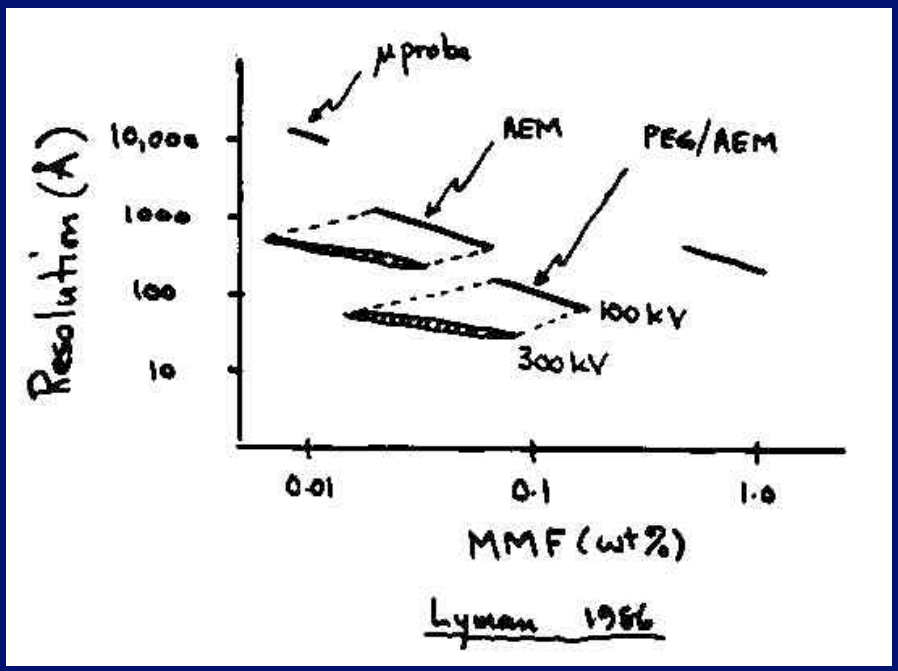

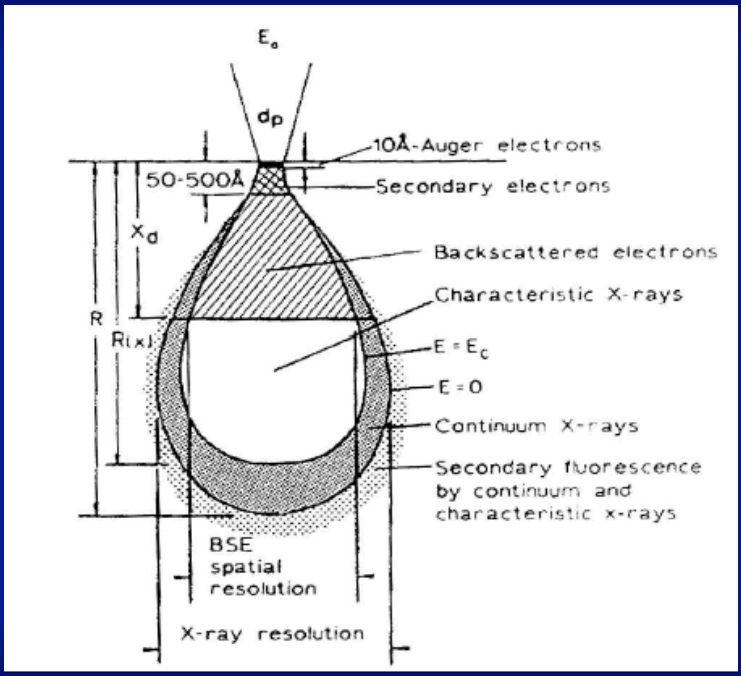

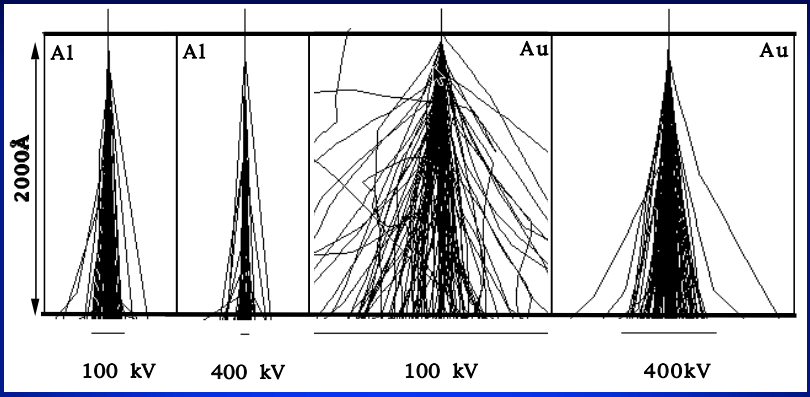

Monte Carlo Calculations of B (Newbury & Myklebust -1979)

Element	Z	Thickness 10nm	50nm	100nm	500nm
Carbon	6	0.22	1.9	4.1	33.0
Aluminium	13	0.41	3.0	7.6	66.4
Copper	29	0.78	5.8	17.5	244.0
Gold	79	1.71	15.0	52.2	1725.0

Analytic Formulation (Elastic Scattering - Goldstein etal 1977)

$$\mathcal{B} = 625 \frac{Z}{E_o} \sqrt{\frac{\rho}{A}} \; t^{3/2}$$

b= Beam Broadening [cm]
E_o= Accelerating Voltage [kV]
A= Atomic Weight
Z= Atomic Number
ρ = Density [gms/cm^3]
t = Thickness [cm]

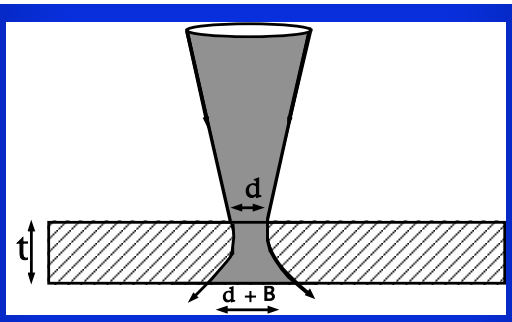

Element	Z	10nm	50nm	100nm	500nm
Carbon	6	0.16	1.8	5.13	57.4
Aluminium	13	0.26	1.9	8.12	90.9
Copper	29	0.68	7.6	21.4	*
Gold	79	15.5	17.3	*	*

*model invalid at higher kV and/or high scattering angles

Data Analysis and Quantification:

Spectral Processing
Thin Film Quantification Methods
Specimen Thickness Effects:
- Absorption
- Fluorescence

Spectral Processing : XEDS

Spectrum = Characteristic Peaks + Background

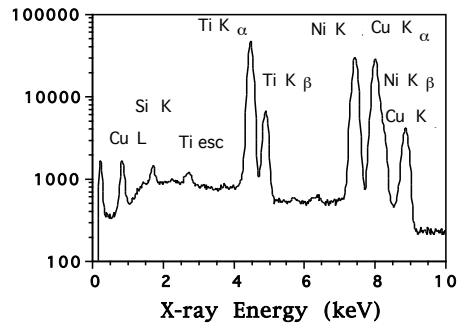

Data Reduction

Simple: Linear Background Fit & Integration

Curve Fitting: Non-Linear Background & Profile Matching

Frequency (Digital) Filtering: Background Suppression & Reference Spectra Fitting

Deconvolution: Fourier Method for Resolution Enhancement

Background Modeling

Simple - Linear and/or Polynominal Interpolation

Modeling - Parametric Fits of Analytic Expressions
Phenomenological Expressions
Modified Bethe Heitler Model
Digital Filtering - Mathematical Supression

Spectral Processing : XEDS
Simple Data Reduction

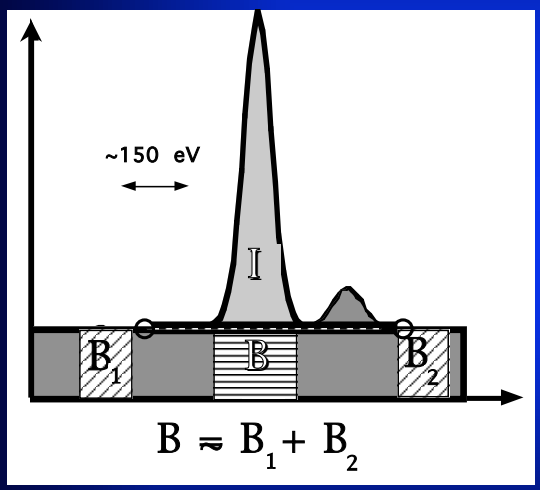

Note: Must use peak integrals (I) and not peak amplitudes (A)

Recall that for a Gaussian Peak

$$I = \int_{-\infty}^{+\infty} A \exp\left(\frac{-x^2}{2\sigma^2}\right) dx = \sqrt{2\pi}\,\sigma\,A$$

Hence for the ratio of Intensities

$$\frac{I_1}{I_2} = \frac{\sigma_1 * A_1}{\sigma_2 * A_2} \neq \frac{A_1}{A_2}$$

Spectral Processing :
XEDS

Background Modeling :
Power Law/Parametric
Fits

$$\text{Bgnd} = \varepsilon^{*}\left(A\left(\frac{E-E_o}{E}\right)^2 + B\left(\frac{E-E_o}{E}\right) + C\right)$$

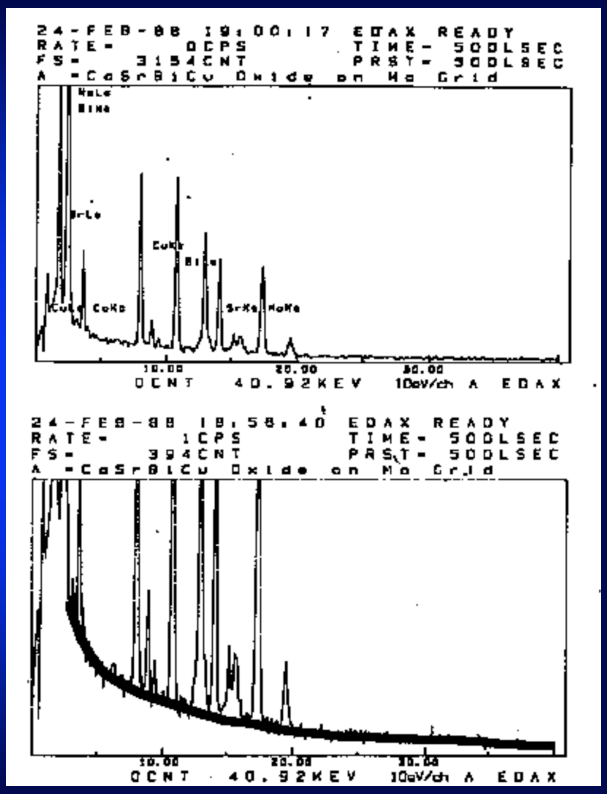

Spectral Processing : XEDS
Digital Filtering

Background Suppression by Mathematical modeling
- Replace Data by new spectra formed by the following linear operation.

$$G(x_i) = [F(x_{+1}) - 2*(\frac{W_-}{W_+})* F(x_0) + F(x_{-1})] \quad \text{where } F(x_j) = \Sigma f(x_j)$$

First Order (Top Hat) Digital Filter

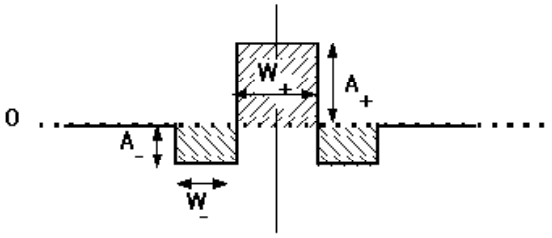

Operator independent
Introduces severe spectral distortion

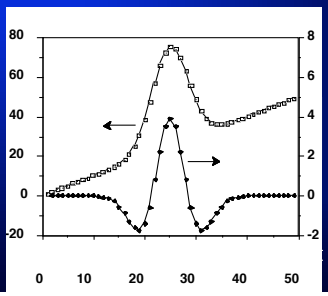

Spectral Processing : XEDS
Digital Filtering

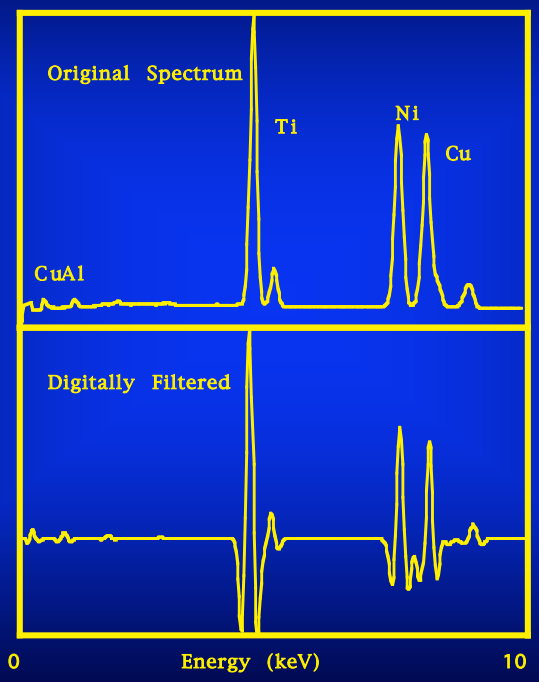

X-ray Production

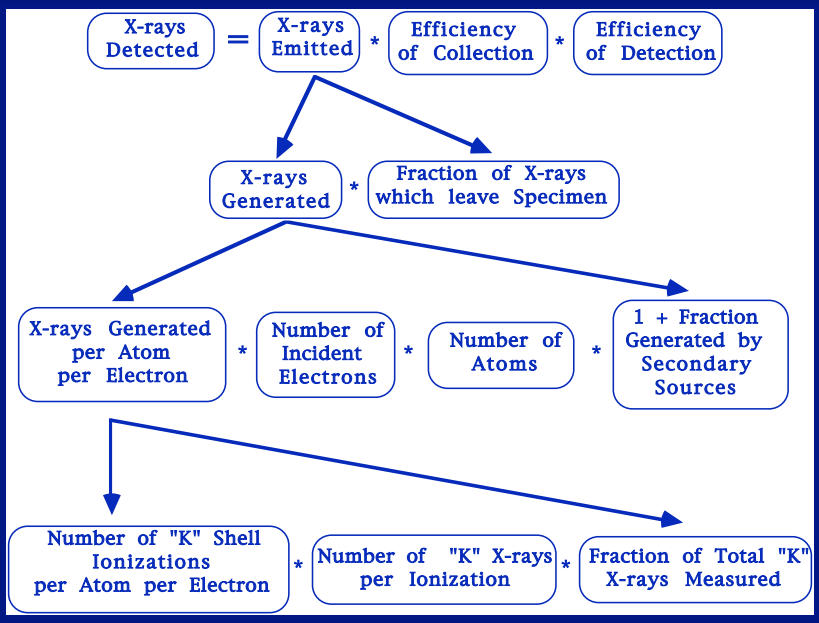

Quantitative Analysis using XEDS

For a thin specimen

$$I_A^{K\alpha} = \{\sigma_A(E,Z)\Gamma_A\omega_A\}C_A\left\{\frac{N_o\rho}{W_A}\right\}\{\eta_o\, t\}\{\varepsilon_A\,\Omega\}$$

I_A	=	Measured x-ray intensity per unit area
σ	=	K^{th}-shell ionization cross-section
ω	=	K^{th}-shell fluorescence yield
Γ	=	K^{th}-shell radiative partition function
W	=	Atomic Weight
N_o	=	Avagodro's number
ρ	=	Density
C	=	Composition (At %)
η_o	=	Incident electron flux
t	=	Specimen thickness
ε	=	Detector efficiency
Ω	=	Detector solid angle

Ionization Cross-Section

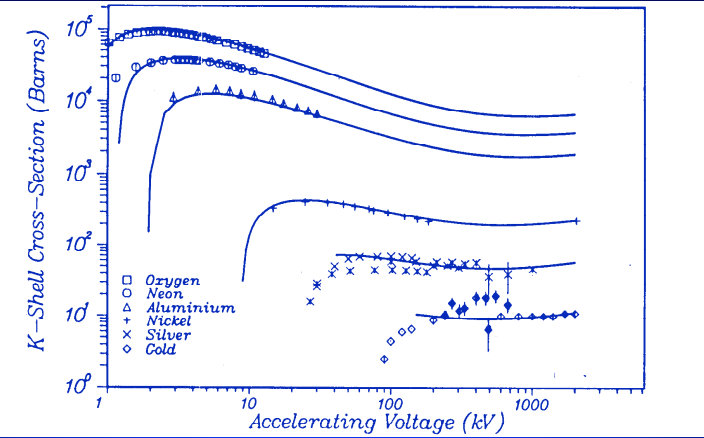

For K Shells

$$Q_K = \frac{a_K * b_K * \left\{ \ln\left(c_K * \frac{T_o}{E_c}\right) - \ln(1-\beta^2) - \beta^2 \right\}}{T_o * E_c}$$

$T_o = 1/2\, m_o c^2 \beta^2$, E_c = Shell Excitation Energy, $\beta = v/c$

For L Shells

$$Q_L = \frac{a_L * b_L * \left\{ \ln\left(c_L * \frac{T_o}{E_c}\right) - \ln(1-\beta^2) - \beta^2 \right\}}{T_o * E_c}$$

X-ray Fluorescence Yield has Systematic Variation With Atomic Number

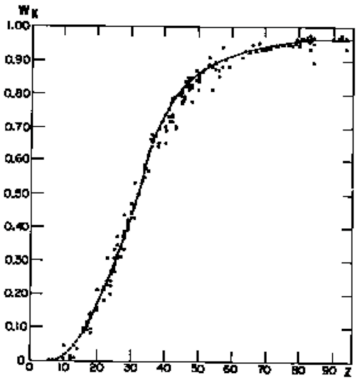

ω_K shell

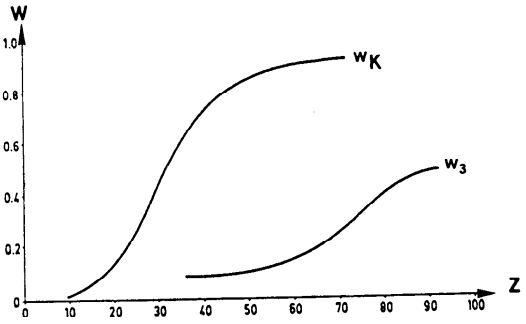

ω_K vs ω_L shell

Relative Intensities of Major X-ray Lines

$$I_K = I_{K\alpha} + I_{K\beta}$$
$$I_L = I_{L\alpha} + I_{L\beta} + I_{L\iota} + I_{L\eta} + I_{L\gamma}$$
$$I_M = I_{M\alpha} + I_{M\beta}$$

Line	Initial	Final	Line	Initial	Final	Line	Initial	Final
$K_{\alpha 1}$ =>	L_3	K	$L_{\alpha 1}$ =>	M_5	L_3	$M_{\alpha 1}$ =>	N_7	M_5
$K_{\alpha 2}$ =>	L_2	K	$L_{\alpha 2}$ =>	M_4	L_3	$M_{\alpha 2}$ =>	N_6	M_5
$K_{\beta 1}$ =>	M_3	K	$L_{\beta 1}$ =>	M_4	L_2	M_β =>	N_6	M_4
$K_{\beta 2}$ =>	N_2	K	$L_{\beta 2}$ =>	N_5	L_3	M_γ =>	N_5	M_3
$K_{\beta 3}$ =>	M_2	K	$L_{\beta 3}$ =>	M_3	L_1			
			$L_{\beta 4}$ =>	M_2	L_1			
			$L_{\gamma 1}$ =>	N_4	L_2			
			$L_{\gamma 3}$ =>	N_3	L_1			
			L_η =>	M_1	L_2			
			L_ι =>	M_1	L_3			

Radiative Partition Function (Γ) Governs the Relative Intensities
Nominal Values (Varies slowly with Atomic Number)

K Shell	L Shell	M Shell
$K_{\alpha 1}$ = 100	$L_{\alpha 1}$ = 100	$M_{\alpha 12}$ = 100
$K_{\alpha 2}$ = 50	$L_{\alpha 2}$ = 50	M_{β} = 60
$K_{\beta 1}$ = 15-30	$L_{\beta 1}$ = 50	
$K_{\beta 2}$ = 1-10	$L_{\beta 2}$ = 20	
$K_{\beta 3}$ = 6-15	$L_{\beta 3}$ = 1-6	
	$L_{\beta 4}$ = 3-5	
	$L_{\gamma 1}$ = 1-10	
	$L_{\gamma 3}$ = 0.5-2	
	L_{η} = 1	
	L_{ι} = 1-3	

Quantitative Analysis using XEDS
Standardless Method

Invoke the Intensity Ratio Method, that is consider the ratio of x-ray lines from two

$$\frac{I_A}{I_B} = \frac{\kappa_A}{\kappa_B}\frac{\varepsilon_A}{\varepsilon_B}\frac{C_A}{C_B} = k_{AB}^{-1}\frac{C_A}{C_B}$$

$$\kappa_A = \frac{\sigma_A \omega_A \Gamma_A}{W_A}$$

$$\frac{\kappa_A}{\kappa_B}\frac{\varepsilon_A}{\varepsilon_B} = k_{AB}^{-1} \quad \text{(k-factor)}$$

This simple equation states that the relative intensity ratio of any two characteristic x-ray lines is directly proportional to the relative composition ratio of their elemental components multiplied by some "constants" and is independent of thickness.

NOTE: **The k_{AB} factor is not a universal constant!! Only the ratio of κ_A/κ_B is a true physical constant and is independant of the AEM system. The ratio of $\varepsilon_A/\varepsilon_B$ is not a constant since no two detectors are identical over their entire operational range. This can cause problems in some cases as we shall see.**

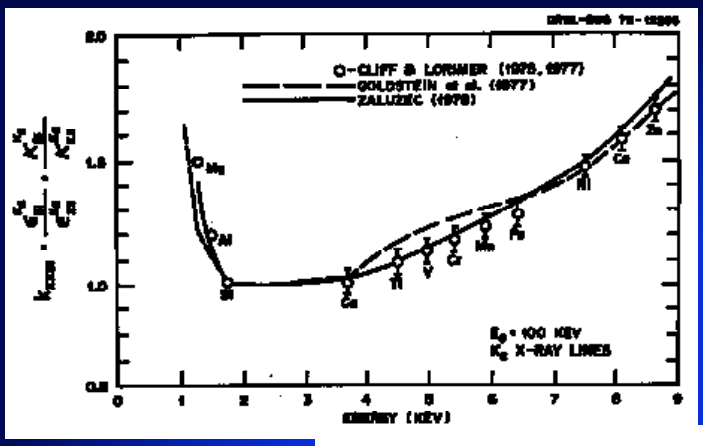

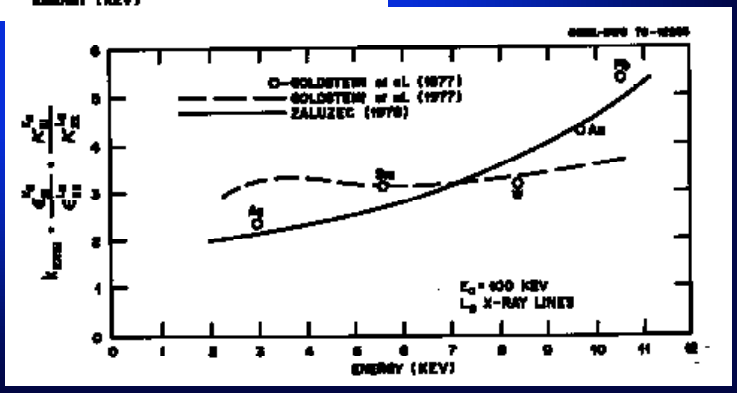

The analysis to this point has only yielded the **relative compositions** of the specimen. We need one additional assumption to convert the relative intensity ratio's (I_i/I_j) into compositons namely:

$$\sum_{i=1}^{N} C_i = 1.0$$

One now has a set of N equations and N unknowns which be solved algebraically solved for the individual composition values.

Thus for a simple two element system we have:

$$\frac{I_A}{I_B} = k_{AB}^{-1} \frac{C_A}{C_B}$$

and

$$C_A + C_B = 1.$$

or

$$C_B \left(\frac{C_A}{C_B} + 1\right) = 1$$

Soving for C_B and C_A

$$C_B = \left(\frac{1}{\left(1+\frac{C_A}{C_B}\right)}\right) = \left(\frac{1}{\left(1+\frac{I_A}{I_B} * k_{AB}\right)}\right) \quad \text{and} \quad C_A = C_B - 1$$

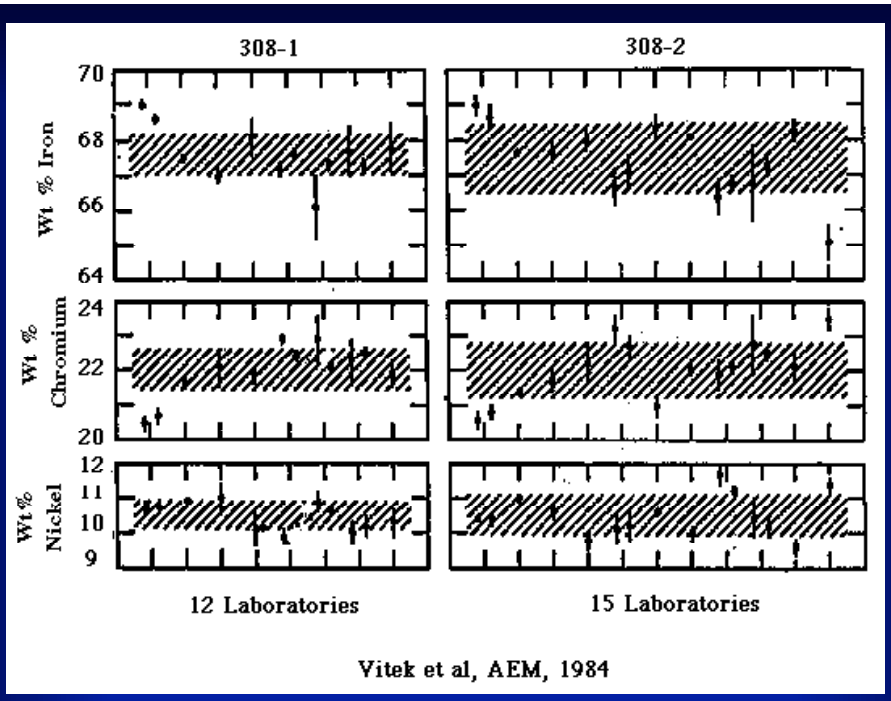

Variation in Measured Composition on 308 SS for Different Labs

Example in which K-factor is stable
Cr, Fe, Ni
Note: Detector efficiency ~ 100% in this energy range

Variation in K-factor with AEM/Detector System
Specimen: Uniform NiO film on Be Grid

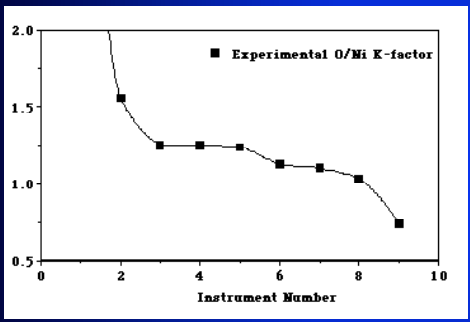

Instrument	Experimental K -Factor	Apparent Variation in Composition
1	5.17	80.9/19.1
2	1.56	56.1/43.9
3	1.25	50.6/49.4
4	1.25	50.6/49.4
5	1.24	50.4/49.5
6	1.13	48.1/51.9
7	1.10	47.4/52.6
8	1.03	45.8/54.2
9	0.74	37.8/62.2

From: Comparison of UTW/WL X-ray Detectors on TEM/STEMs and STEMs

Thomas, Charlot, Franti, Garratt-Reed, Goodhew, Joy, Lee, Ng, Plicta, Zaluzec.
Analytical Electron Microscopy-1984

Variation in K-factor with AEM/Detector System

Low Energy End will not be the only problematic area

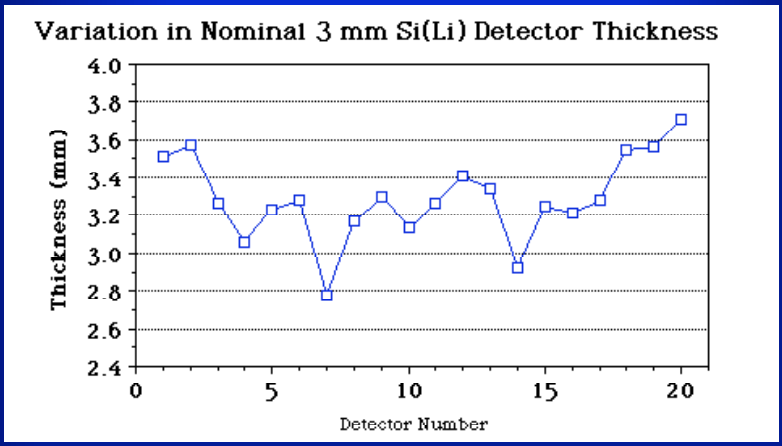

Determining the k_{AB}^{-1} Factor

Experimental Measurements

Prepare thin-film standards of known composition
then measure relative intensities and solve explicitly
for the k_{AB} factor needed. Prepare a working data base.

This is the "best" method, but
- specimen composition must be verified independently
- must have a standard for every element to be studied

Theoretical Calculations

Attempt first principles calculation knowing
some fundamental parameters of the AEM system

Start with a limited number of kAB factor measurements,
then fit the AEM parameters to best match the data.
Extrapolate to systems where measurements and/or
standards do not exist.

- **Method 1**. (Goldstein etal) Assume values for Γ,ω,ε and determine the best s to fit k_{AB}. This procedure essentially iterates the fit of s to the data.

Method 2. (Zaluzec) Assume values for Γ,ω,σ determine the best e to fit k_{AB}. This procedure essentially iterates the fit of e (detector window parameters) to the data.

K-Factor Calculation
Experiment
vs
Theory

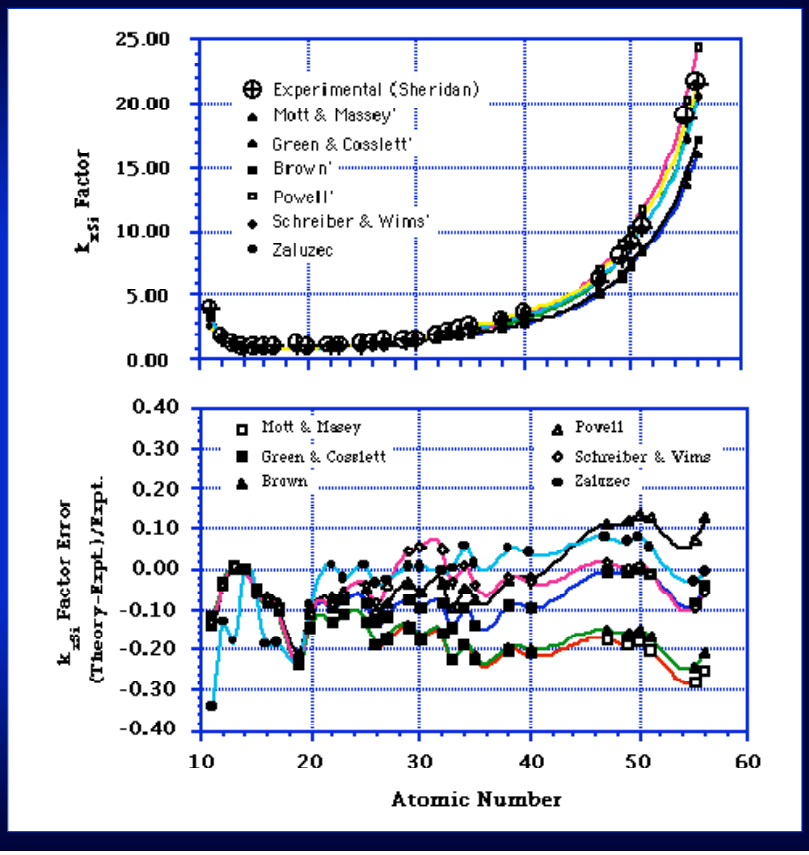

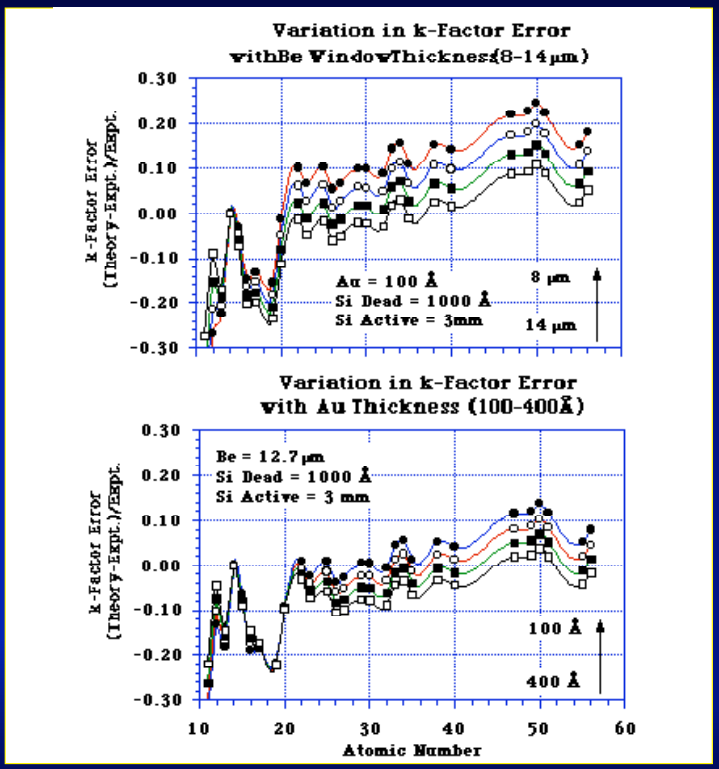

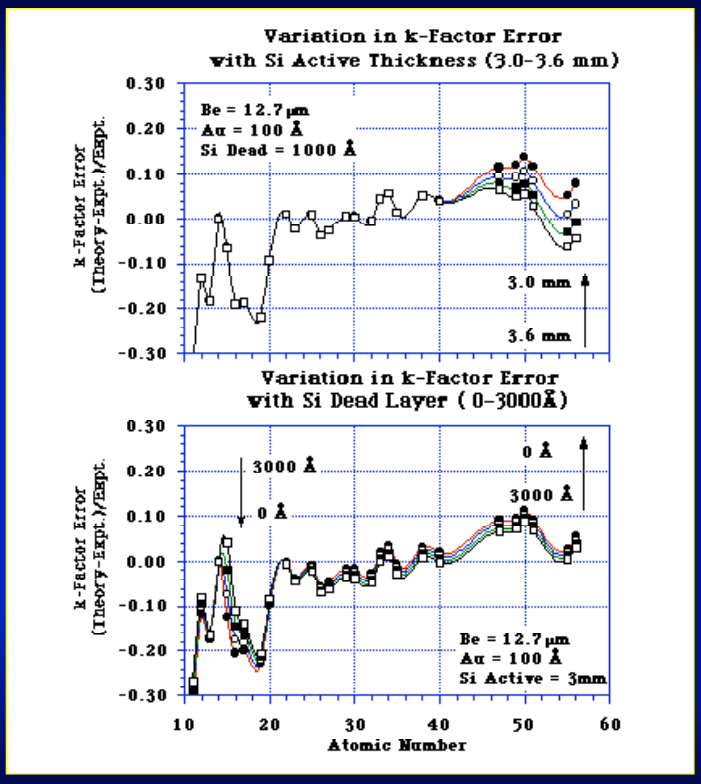
Variation in k-Factor Error
with Si Active Thickness (3.0-3.6 mm)
Be = 12.7 µm
Au = 100 Å
Si Dead = 1000 Å
3.0 mm
3.6 mm
k-Factor Error
(Theory-Expt.)/Expt.
Variation in k-Factor Error
with Si Dead Layer (0-3000Å)
3000 Å
0 Å
0 Å
3000 Å
Be = 12.7 µm
Au = 100 Å
Si Active = 3mm
Atomic Number

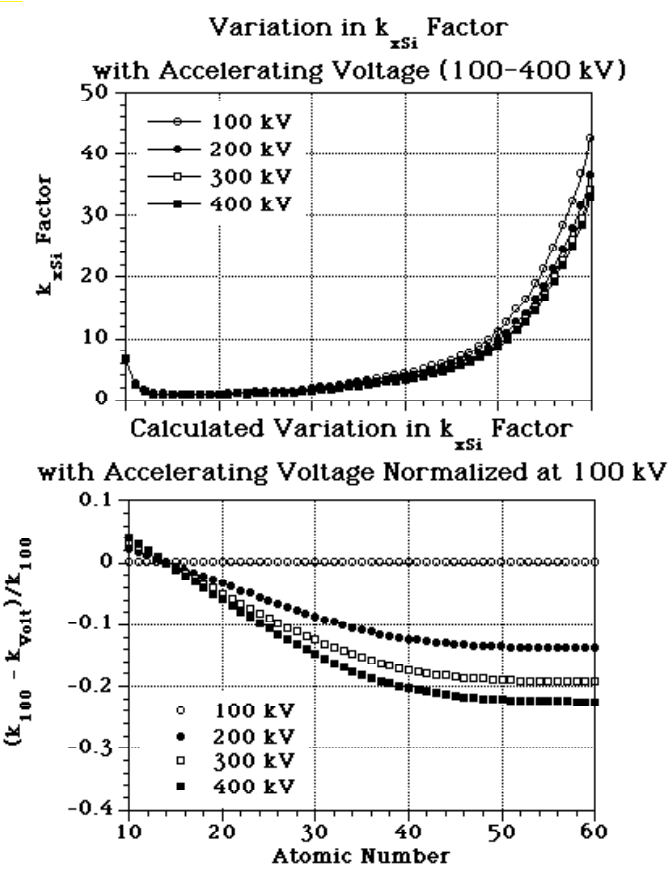
Variation in k xSi Factor
with Accelerating Voltage (100-400 kV)
100 kV
200 kV
300 kV
400 kV
k xSi Factor
Calculated Variation in k xSi Factor
with Accelerating Voltage Normalized at 100 kV
(k 100 - k Volt)/k 100
100 kV
200 kV
300 kV
400 kV
Atomic Number

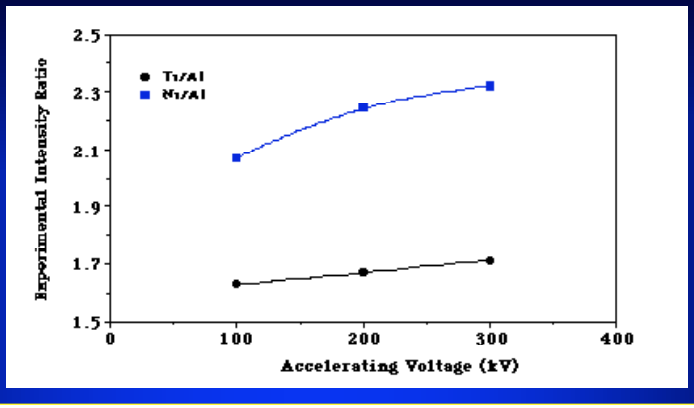

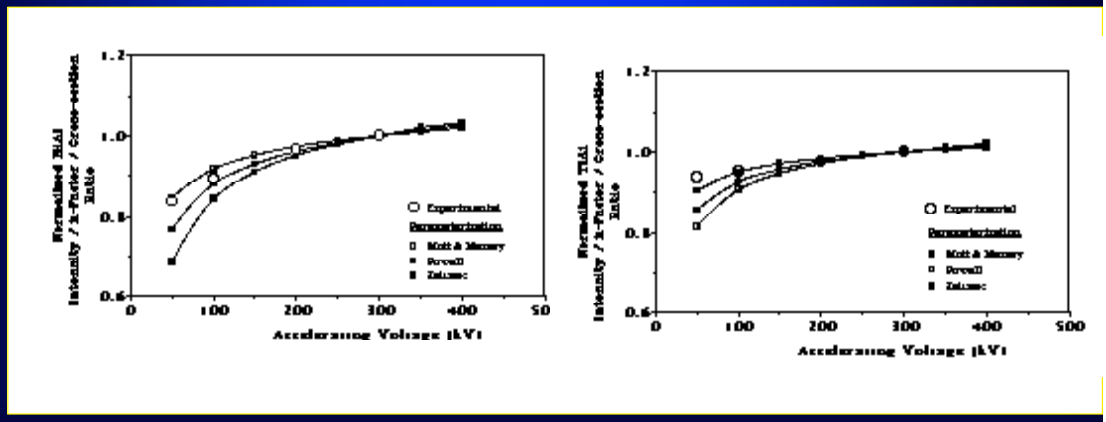

Sources of values for k_{AB} Calculations

W - International Tables of Atomic Weights

Γ(K) - Schreiber and Wims , X-ray Spectroscopy (1982) Vol 11, p. 42

Γ(L) - Scofield, Atomic and Nuclear Data Tables (1974) Vol 14, #2, p. 121

ω (K) - Bambynek etal, Rev. Mod. Physics, Vol 44, p. 716
Freund, X-ray Spectrometry, (1975) Vol 4, p.90

ω(L) - Krause, J. Phys. Chem. Ref. Data (1974) Vol 8, p.307

σ(Eo) - Inokuti, Rev. Mod. Physics, 43, No. 3, 297 (1971)
- Goldstein etal, SEM 1, 315, (1977)
- Chapman etal, X-ray Spectrometry, 12,153,(1983)
- Rez, X-ray Spectrometry, 13, 55, (1984)
- Egerton, Ultramicroscopy, 4, 169, (1969)
- Zaluzec, AEM-1984, San Fran. Press. 279, (1984)

ε (E) - Use mass absorption coefficients from:
-Thinh and Leroux; X-ray Spect. (1979), 8, p. 963
-Henke and Ebsiu, Adv. in X-ray Analysis,17, (1974)
-Holton and Zaluzec, AEM-1984, San Fran Press,353,(1984)

Quantitative Analysis using XEDS
Thin Film Standards Method

Invoke the Intensity Ratio Method, but now consider the ratio of the same x-ray line from two different specimens, where one is from a **standard** of known composition while the other is **unknown**:

$$\frac{I_u}{I_s} = \frac{\eta_u \rho_u t_u}{\eta_s \rho_s t_s} * \frac{C_u}{C_s}$$

$$C_u = \frac{\eta_s \rho_s t_s}{\eta_u \rho_u t_u} * \frac{I_u}{I_s} * C_s$$

This simple equation states that the relative intensity ratio of same characteristic x-ray line is directly proportional to the relative composition ratio of the two specimens multiplied by a some new parameters.

η = incident beam current
ρ = local specimen density
t = local specimen thickness

Quantitative Analysis using XEDS
Specimen Thickness Effects

For finite thickness specimens, what is a thin film?

Previous Assumptions:
No Energy loss,
No X-ray absorption,
No X-ray fluorescence

NOTE: Electron Transparency is insufficient!

Effects of energy loss on Characteristic X-ray Production:

$$I_A = \frac{N_O \rho C_A}{W_A} \omega_A \Gamma_A \eta_o \Omega \varepsilon_A \int_o^{t_o} \sigma_A(E) \, dt$$

Quantitative Analysis using XEDS : Absorption Correction

$$I = \int_0^{t_o} I_o(t)\ \exp\ (-\mu^* d)\ dt = \int_0^{t_o} I_o(t)\ \exp\ (-\chi\rho t)\ dt$$

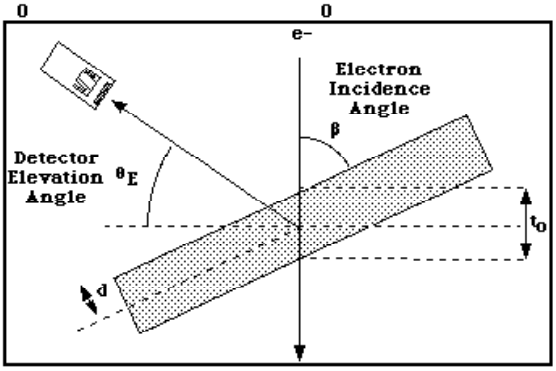

d = Absorption Pathlength from the specimen to detector

$$= t\,\frac{\sin(\beta)}{\cos(\beta-\theta_E)}$$

χ = Geometrical factor multiplied by average mass absorption coefficient for the measured x-ray line in the compound

$$= \left(\frac{\mu}{\rho}\right)_{\text{X in Spec.}} * \frac{\sin(\beta)}{\cos(\beta-\theta_E)}$$

$\left(\frac{\mu}{\rho}\right)_{\text{X in Spec.}}$ = Weighted average mass absorption coefficient

$$= \sum_{i=1}^{N} \left(\frac{\mu}{\rho}\right)_i * C_i$$ (Note: composition dependent!)

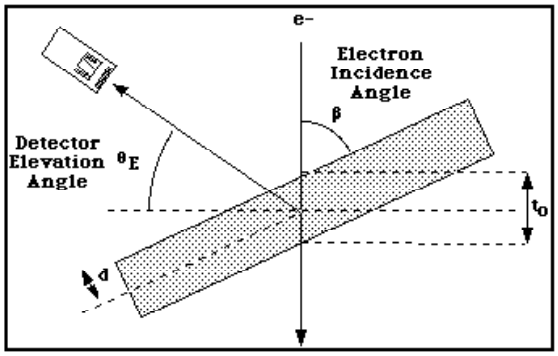

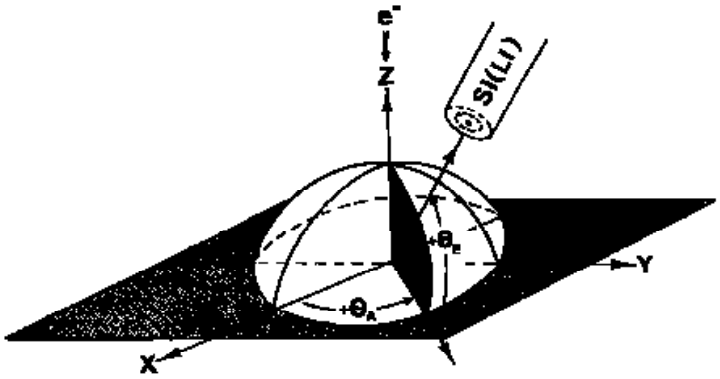

$$\beta = \text{Arccos}\left(\frac{\sin\phi_y \cdot \cos\theta_A \cdot \cos\theta_E + \sin\phi_x \cdot \cos\phi_y \cdot \cos\theta_E \cdot \sin\theta_A}{\sqrt{a^2+b^2+c^2}}\right)$$

$$a = \cos\phi_x \cdot \cos\phi_y \cdot \cos\theta_A \cdot \cos\theta_E$$
$$b = \cos\phi_x \cdot \cos\phi_y \cdot \cos\theta_E \cdot \sin\theta_A$$
$$c = \sin\phi_y \cdot \cos\theta_A \cdot \cos\theta_E + \sin\phi_x \cdot \cos\phi_y \cdot \cos\theta_E \cdot \sin\theta_A$$

Now rederive the standardless equations to include absorption.

$$\frac{I_A}{I_B} = \frac{\varepsilon_A}{\varepsilon_B} * \frac{\kappa_A}{\kappa_B} * \frac{\delta_A}{\delta_B} * \frac{C_A}{C_B}$$

with

$$\frac{\delta A}{\delta B} = \frac{\left(\frac{\mu}{\rho}\right)^{\text{B in AB}}}{\left(\frac{\mu}{\rho}\right)^{\text{A in AB}}} \frac{\left(1 - \exp(-\chi\rho t^*)^{\text{A in}}_{\text{AB}}\right)}{\left(1 - \exp(-\chi\rho t^*)^{\text{B in}}_{\text{AB}}\right)}$$

$$t^* = t_o \frac{\sin(\beta)}{\cos(\beta - \theta_E)}$$

$$\chi = \left(\frac{\mu}{\rho}\right)_{\text{X-ray in Compound}} = \sum_{i=1}^{N} \left(\frac{\mu}{\rho}\right)_i * C_i$$

β = Electron Incidence Angle
= Function of Stage Tilts: ϕ_x, ϕ_y, & Detector Azimuth θ_A)

θ_E = Detector Elevation Angle

Define the Thin Film approximation: $\chi\rho t^* < 0.1$

Thin Film approximation: $\chi\rho t^* < 0.1$

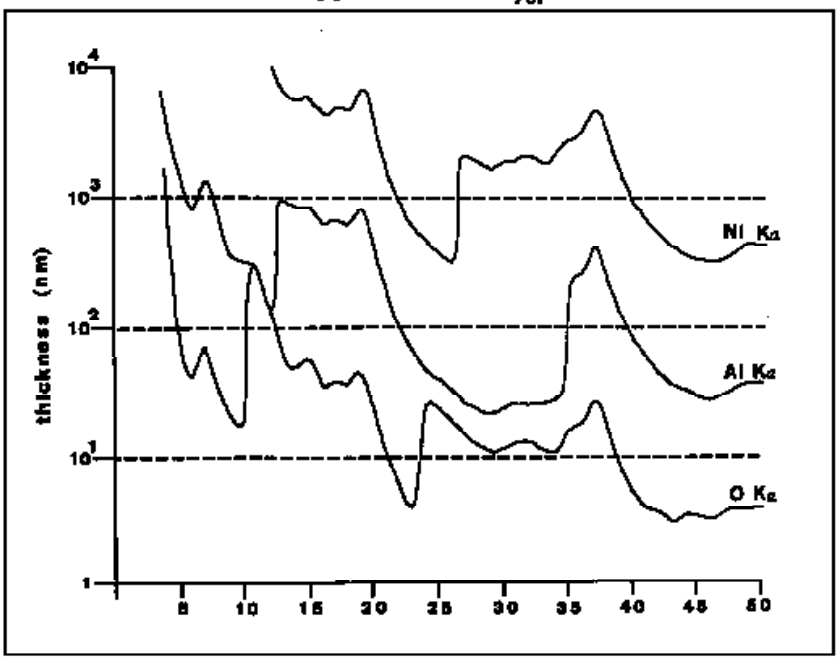

$$t^* \leq \frac{0.1}{\chi\rho}$$

Effect of Tilting Specimen on Absorption

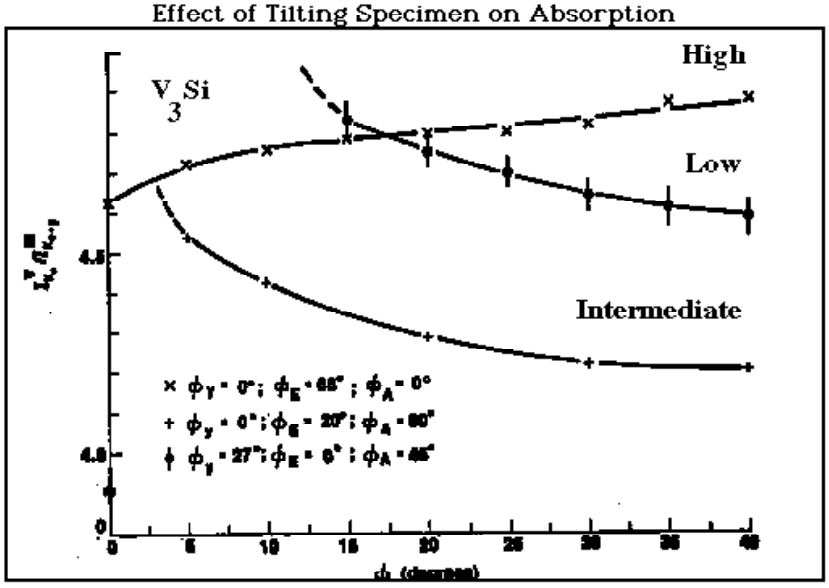

For a plane paralle slab specimen, tilting has the effect of increasing the Specimen Thickness.
Different Detector/Specimen Geometries will enhance/reduce the Absorption Effects

In the "real" world few specimens have the shape used to derive this correction. Next consider two representative geometries:

Symmetric Wedge Geometry:

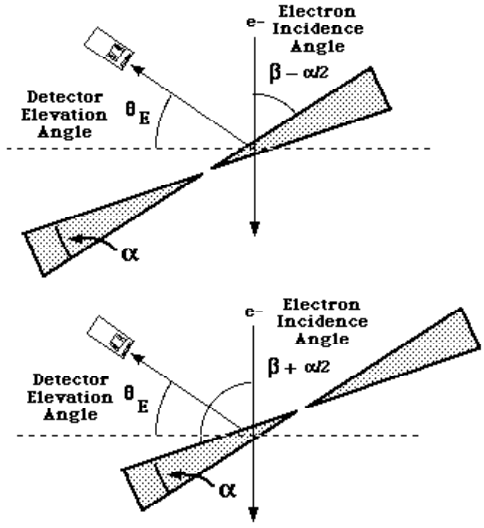

Replace all **β**'s by $\beta \pm \alpha/2$, where **α** is the wedge angle of the specimen

$+\alpha/2$ variant applies when the detector is positioned such that the pathlength ***increases*** relative to the parallel slab model

$-\alpha/2$ variant applies when the detector is positioned such that the pathlength ***decreases*** relative to the parallel slab model

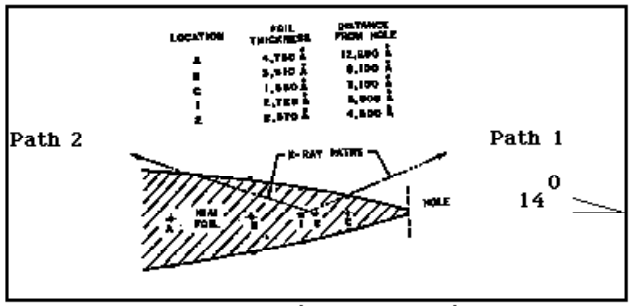

Glitz etal (MAS-1981)

Attempt a Wedge Model Correction using previous formulae.

Path #1	Path #2
$\frac{I_{Ni}}{I_{Al}} = 2.64$	$\frac{I_{Ni}}{I_{Al}} = 5.18$
Thin Film Model $\frac{Ni=60.9}{Al=39.1}$	Thin Film Model Error!
Parallel Slab $\frac{Ni=45.3}{Al=54.7}$	Parallel Slab $\frac{Ni=60.5}{Al=39.5}$
Wedge Model $\frac{Ni=50.6}{Al=49.4}$	Wedge Model $\frac{Ni=42.6}{Al=57.4}$
χ pt Ni = 0.016	χ pt Ni = 0.081
χ pt Ni = 0.925	χ pt Ni = 4.24

Absorption Correction has limited applications keep χ pt < 1

Specimen Homogenity

In this and all other derivations we have assumed that over the excited volume, as well as along th exiting pathlength, the specimen is homogeneous in composition. If this assumption is invalid, one must reformulate the absorption correction and take into account changes in : μ/ρ, ρ, and t along the exiting pathlength.

Effects of Beam Broadening

Parallel Slab Model: No Change in absorption pathlength
Wedge Model: There is a correction the magnitude of which varies with the wedge angle.

Effects of Irregular Surface

This cannot be analytically modeled but must be understood!

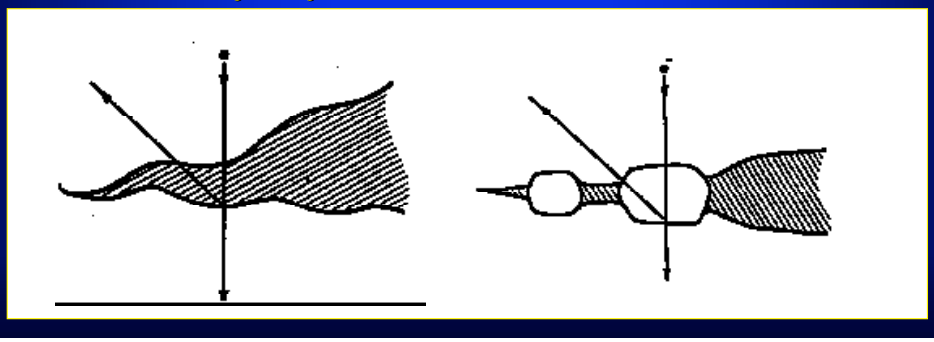

X-Ray Fluorescence Correction

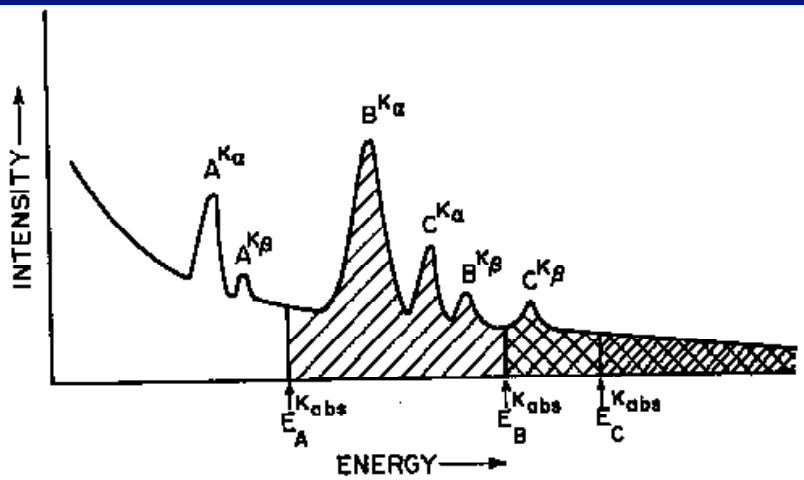

$$I_A^{Measured} = I_A^{Electron} + I_A^{XRF\ by\ B}$$

$$I_A^{Measured} = I_A^{Electron}\left(1 + \frac{I_A^{XRF\ by\ B}}{I_A^{Electron}}\right)$$

Next rederive the standardless equations to include x-ray fluorescence and you can show.

$$\frac{I_A}{I_B} = \frac{\varepsilon_A}{\varepsilon_B} * \frac{\kappa_A}{\kappa_B} * \frac{\delta_A}{\delta_B} * \frac{\gamma_A}{\gamma_B} * \frac{C_A}{C_B}$$

as in the case of x-ray absorption this requires iterative solution because the ratio of γ's are composition dependent..

When is the XRF Correction important?

- When fluorescing line is near the absorption edge of the lower energy line. Typically within a few atomic numbers (i.e. Z+2 to Z+6)
- When specimen is thick or path length is long

Define a thin film approximation for XRF as:

$$\frac{I_A^{\text{XRF by i}}}{I_A^{\text{Electron}}} < 0.05$$

$$C_i\ \omega_i\ \Gamma i\ \frac{A_A}{A_i}\ \frac{Q_i}{Q_A}\left(\frac{\Delta\mu}{\mu}\right)_A\ \left(\frac{\mu^i}{\rho}\right)_A \frac{\rho T}{2}\left[1.12 + \left(\frac{\mu^i}{\rho}\right)_{Ai} \bullet \frac{\rho T}{4} - \ln\left(\left(\frac{\mu^i}{\rho}\right)_{Ai} \bullet \rho T\right)\right] < 0.05$$

Examples Absorption & Fluorescence Corrections

Assume 100 kV, $\theta_A = 90^o$, $\theta_E = 20^o$, $\beta = 35^o$, $\alpha = 0^o$ i.e. tilted parallel slab

Ni 90%, Fe 10%

Calculation of Thin Film approximation $\chi\rho t$ => 1.25µm for Fe in the Alloy

∴ for TEM specimens we can almost always ignore absorption effects

What about XRF?

Let T = 5000Å $\quad \frac{I_{Fe}^{\text{XRF by Ni}}}{I_{Fe}^{\text{Electron}}} =$ 0.103 i.e. ~10%

Let T = 1000Å $\quad \frac{I_{Fe}^{\text{XRF by Ni}}}{I_{Fe}^{\text{Electron}}} =$ 0.028 i.e. 2.8%

∴ for TEM specimens we may be affected by XRF

Ni 90%, Al 10%

Calculation of Thin Film approximation $\chi\rho t$ => 232 Å for Al in Alloy!!!

$\therefore$ for TEM specimens we cannot ignore absorption effects

What about XRF?

Let T = 5000Å $\quad \frac{I_{Al}^{\text{XRF by Ni}}}{I_{Al}^{\text{Electron}}} =$ 0.000186 i.e. 0.01%

$\therefore$ for typical TEM specimens we can ignore XRF effects

Additional Topics

Heterogeneous Specimens
Composition Profiles
Electron Channeling
Radiation Damage

All quantitative analysis equations were derived assuming that the specimen is homogeneous over the exited volume

Application of the these equations to heterogenous specimens effectively averages the composition over the excited volume.

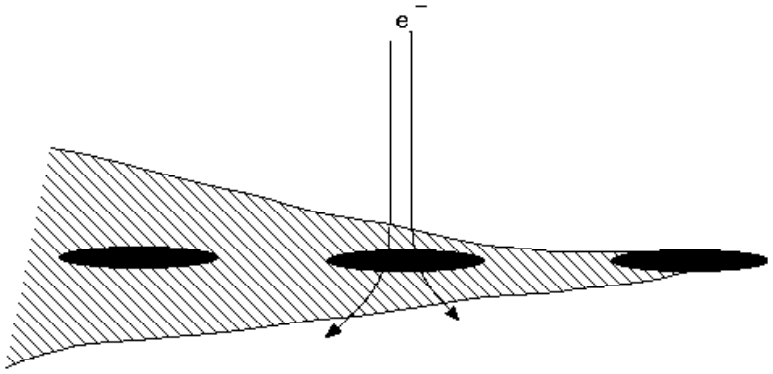

Grain Boundary Segregation

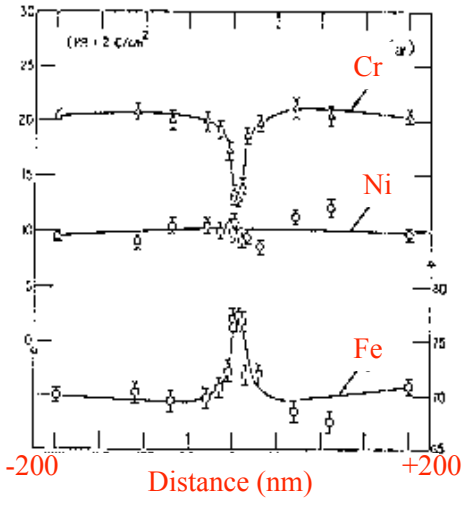

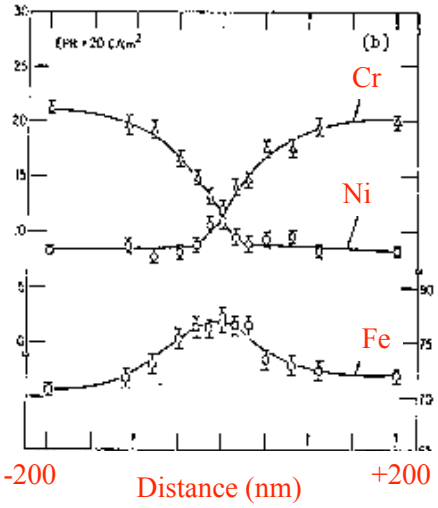

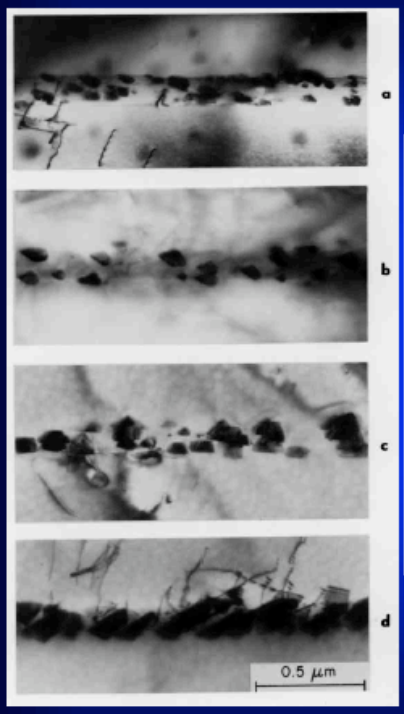

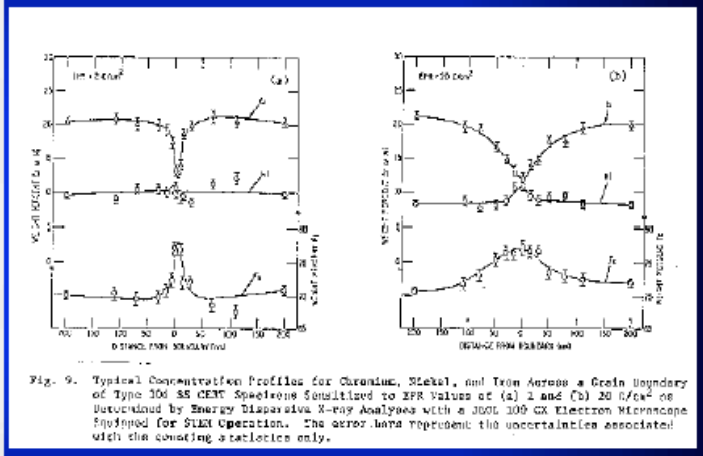

Fig. 9. Typical Concentration Profiles for Chromium, Nickel, and Iron Across a Grain Boundary of Type 304 SS CEMT Specimens Sensitized to EPR Values of (a) 1 and (b) 20 C/cm² as Determined by Energy Dispersive X-ray Analyses with a JEOL 100 CX Electron Microscope Equipped for STEM Operation. The error bars represent the uncertainties associated with the counting statistics only.

$$C^*(x,y) = C(x,y,z)^* \, d(x,y,z)$$

$C^*(x,y)$ = Apparent profile measured
$C(x,y,z)$ = Actual composition profile
$d(x,y,z)$ = Incident beam profile

$*$ = Convolution operator

F, F^{-1} = Fourier and Inverse Fourier Transforms

In the 2 dimensional limit one can deconvolute the measured profile using:

$$C(x,y) = F^{-1}\left\{\frac{F\{C^*(x,y)\}}{F\{d(x,y)\}}\right\}$$

Realistically, it is better to decrease the probe diameter and specimen thickness

Electron Channeling Induced X-ray Emission

- Characteristic X-ray Emission is not truly isotropic in crystalline materials!

- Original Observations of Effect
  - Duncumb '62, Hall '66, Cherns etal '73
- Predicted Applications
  - Cowley '64, '70
- ACHEMI Technique -
  - Tafto '79, Spence & Tafto '83
- Multi-Variate Statistical Analysis -
  - Rossouw etal , Anderson and others late80'-90's

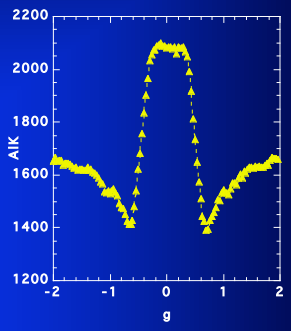

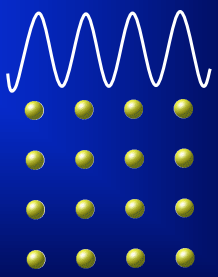

High Angular Resolution Electron Channeling X-ray Spectroscopy

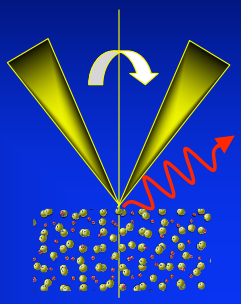

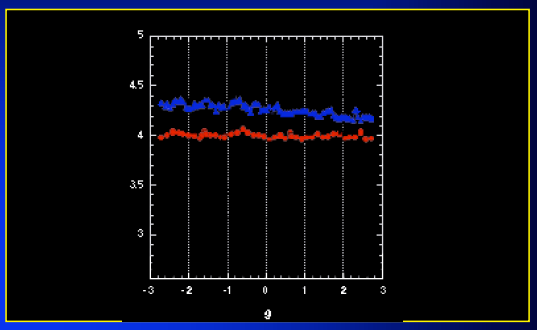

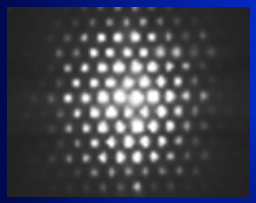

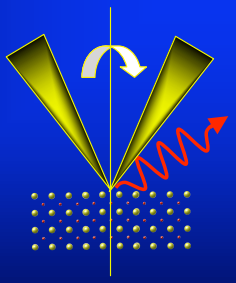

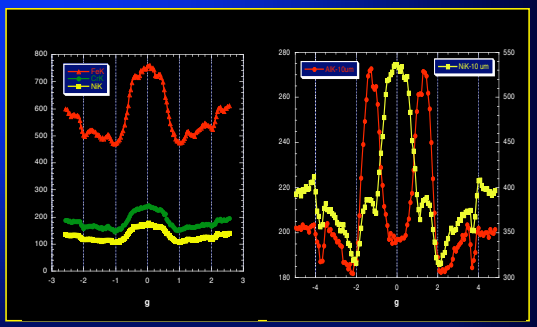

Orientation Dependance in Homogeneous Alloys

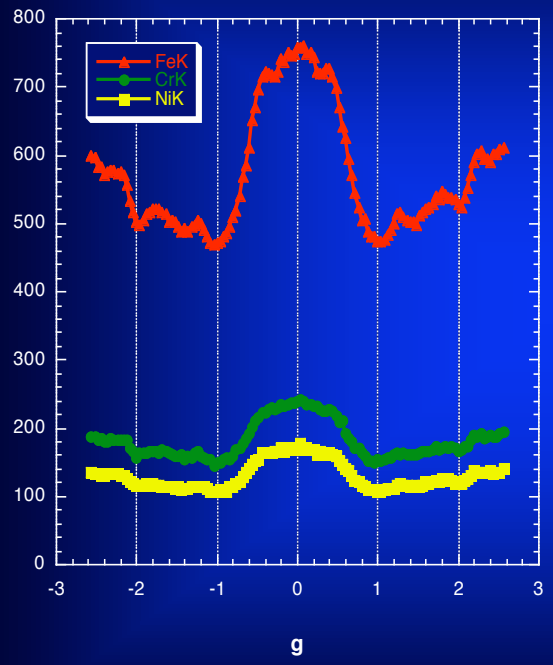

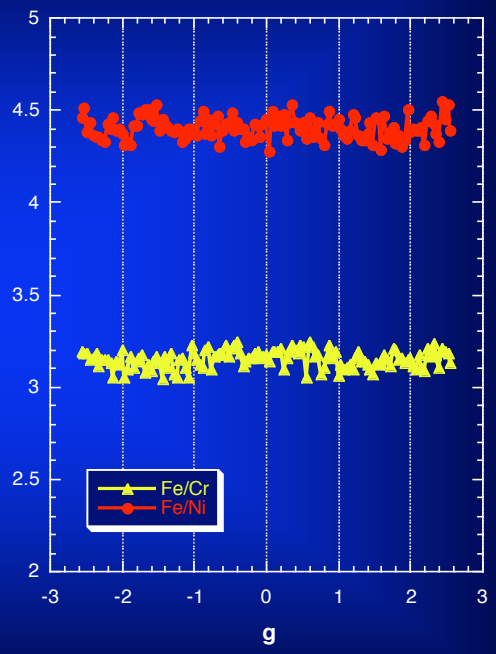

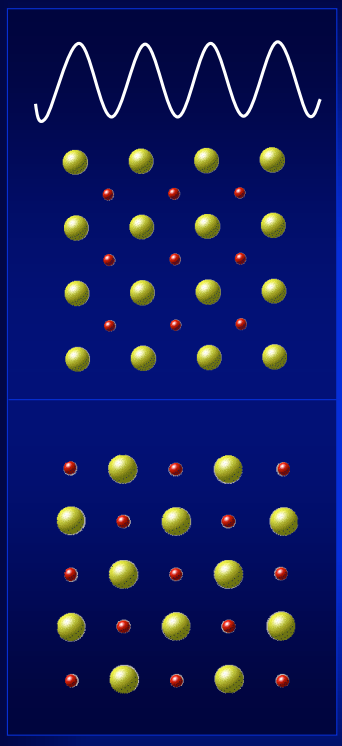

Applications in Ordered Systems

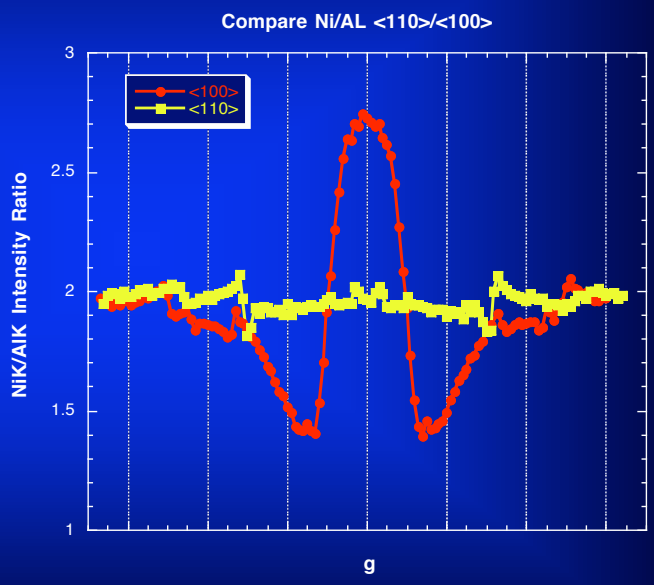

ALCHEMI
Atom Location by CHanneling EMIssion
Tafto & Spence - Science 1982

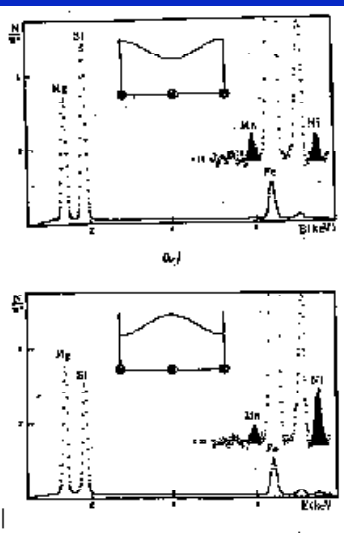

$(Mg_{0.90}Fe_{0.10}Ni_{0.004}Mn_{.002})_2SiO_4$

Note: Mn prefers Si Sites and Ni prefers Mg Sites